Enchemica, LLC
2335 Buckingham Circle
Loveland, CO 80538 USA
1-970-481-9338

TECHNICAL MEMORANDUM

TO: Vicky Peacey, Resolution Copper

FROM: Ted Eary, Enchemica

DATE: June 26, 2018

SUBJECT: Block Cave Geochemical Model – 2018 Update on Calculation Approach and Results

1 INTRODUCTION

The purpose of this technical memorandum is to provide an updated description of the geochemical model of the block cave system. This model has been updated due to revisions in the tailings schedule which now matches the mine schedule (41 years), consideration of geologic information collected since submittal of the Mine Plan of Operations in 2013, and hydrologic modeling predictions of groundwater inflow, which was completed by WSP in 2018 and informed by the EIS groundwater working group.

2 MODELING SEQUENCE

The sequence of models used for predicting water chemistry for the Resolution Project is shown in Figure 2-1. This memo is focused on updates made to the block cave geochemistry model. The block cave geochemistry relies on data from the following models:

- Rates of groundwater flow into the block cave mining zones predicted by the WSP hydrologic model.
- Rates of freshwater inflow for use as mine service water (cooling, dust suppression, drilling, and other miscellaneous uses) from Resolution Copper (Enchemica, 2018a).
- Sulfide oxidation model used to calculate the thickness of the oxidation zone in draw-points (Enchemica, 2018b).

The block cave model produces predictions of water flow and chemistry for sump water pumped from the block cave and water contained in ore moisture. The sump water is comprised of all water expected to be collected in the mine, including cooling blowdown water, excess mine service water, and groundwater. The water making up ore moisture is comprised of mine service water that will be used to spray and cool ore from high temperatures as it is mined and conveyed to the surface. The block cave geochemistry model provides:

- Inputs to the tailings solute geochemistry model

The tailings solute geochemistry model provides inputs to additional models of seepage loss and transport (Figure 2-1).

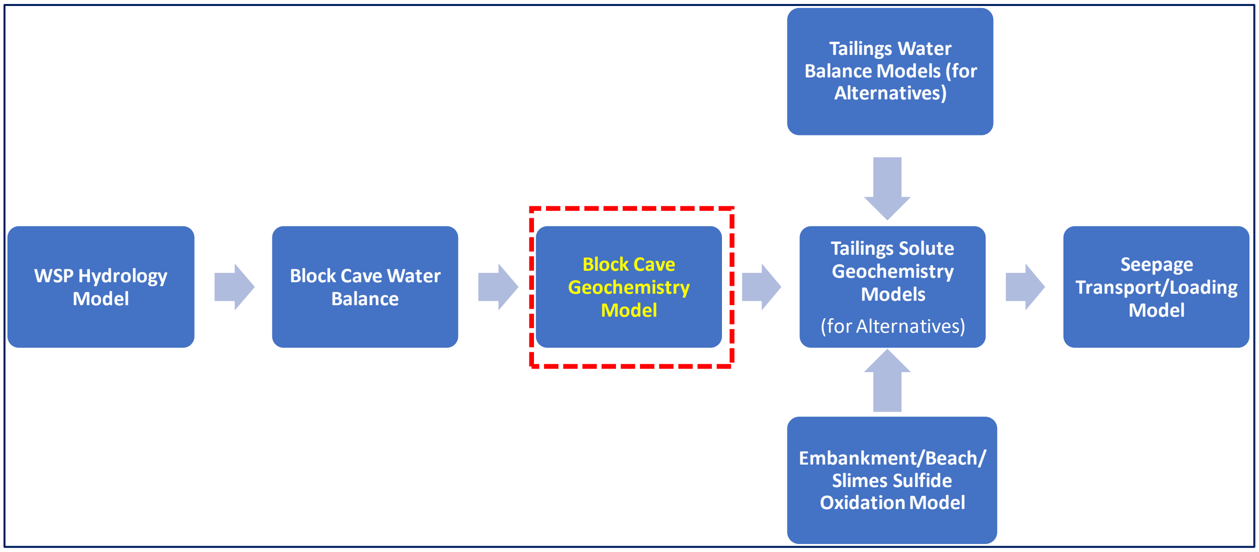

Figure 2-1. Modeling sequence for prediction of water chemistry during mining operations

3 MODELING APPROACH

3.1 Software

The model was developed with a combination of GoldSim (version 12.0) and PHREEQC (Parkhurst and Appelo, 2013). GoldSim was used for the water and chemical mass balance components of the model. PHREEQC was used for the reactive processes that affect water chemistry. The WATEQ4F.DAT thermodynamic database was used for the PHREEQC calculations. This database was modified by the addition of basis species and thermodynamic data for Sb, Be, Co, Cr, Mo, Tl, and V. Thermodynamic data for these elements were obtained from the MINTEQ.V4.DAT database. The chemical portions of the model include calculations for:

- Ca, Mg, Na, K, Cl, HCO_3, SO_4, SiO_2, F, NO_3-N, Al, Sb, As, Ba, Be, B, Cd, Cr, Co, Cu, Fe, Pb, Mn, Mo, Ni, Se, Ag, Tl, Zn, and pH

The PHREEQC geochemical model was integrated directly into the GoldSim water balance model, so that changes to water chemistry resulting from reactive processes are made at each time step in the simulations and incorporated directly into the simulation results (Eary, 2007).

3.2 Simulation Period

The simulation period was 41 years with a 15-day timestep. Most of the input data to the model are on a quarter-year to yearly basis; hence the 15-day timestep was found to be short enough to prevent mass transfer warnings from GoldSim while yielding reasonably short run time. Both the water balance and PHREEQC calculations are conducted at each time step.

3.2.1 Calculation Logic

The calculation logic and sequence for the model is summarized in Figure 3-1. The model contains two main sets of calculation sequences:

- Chemical loads from water sources with static chemistries, including:
  - Groundwater inflow from the Apache Leap Tuff (ALT)
  - Groundwater inflow from the deep system
  - Blowdown water from ventilation and cooling systems
  - Excess mine service water

  These chemical loads are accumulated in the mine sump where they are divided by the rate of water flow and volume of the sump to obtain concentrations. The sump concentrations are equilibrated with geochemical processes with PHREEQC.
- Chemical loads from water sources expected to have dynamic chemistries, including:
  - Oxidation and leaching of ore exposed in draw-points
  - Oxidation and leaching of ore in surface stockpiles

  These chemical loads are created by oxidation and leaching at active draw-points and in the surface stockpile where sulfide ore is exposed to air and water. The primary source of water is expected to be mine service water that is sprayed on ore at the draw-points and on conveyors to cool the ore and suppress dust prior to transport to the surface. For ore in the draw-points, the extent of oxidation and leaching is a function of the depth of O_2 penetration, oxidation and leaching rates at elevated temperatures, and time of exposure to O_2, which is estimated to be 24 h (see below for more detailed discussion of ore residence time). For the stockpile, a similar approach is taken except that is assumed the that mass of ore deposited over 24-h is completely exposed to atmospheric O_2, although at a lower temperature of 33°C due to cooling before being deposited in the stockpile. The chemical composition of ore moisture is equilibrated with various geochemical processes with PHREEQC. As such, the assumption is that 100% of the chemical load from oxidation and leaching at the draw-points and in the stockpile, including the masses of any secondary precipitates is retained in the ore moisture and transported to the mill with the ore. Nominal ore moisture content as provided by Resolution Copper is assumed to be 4% by weight.

This sequence of calculations produces two chemical loads to the West Plant

- Sump water
- Water retained in ore moisture.

Both these sources of water will become a portion of the water used for ore processing with the chemical loads generated in the block cave transferred to the tailings and process water circuit.

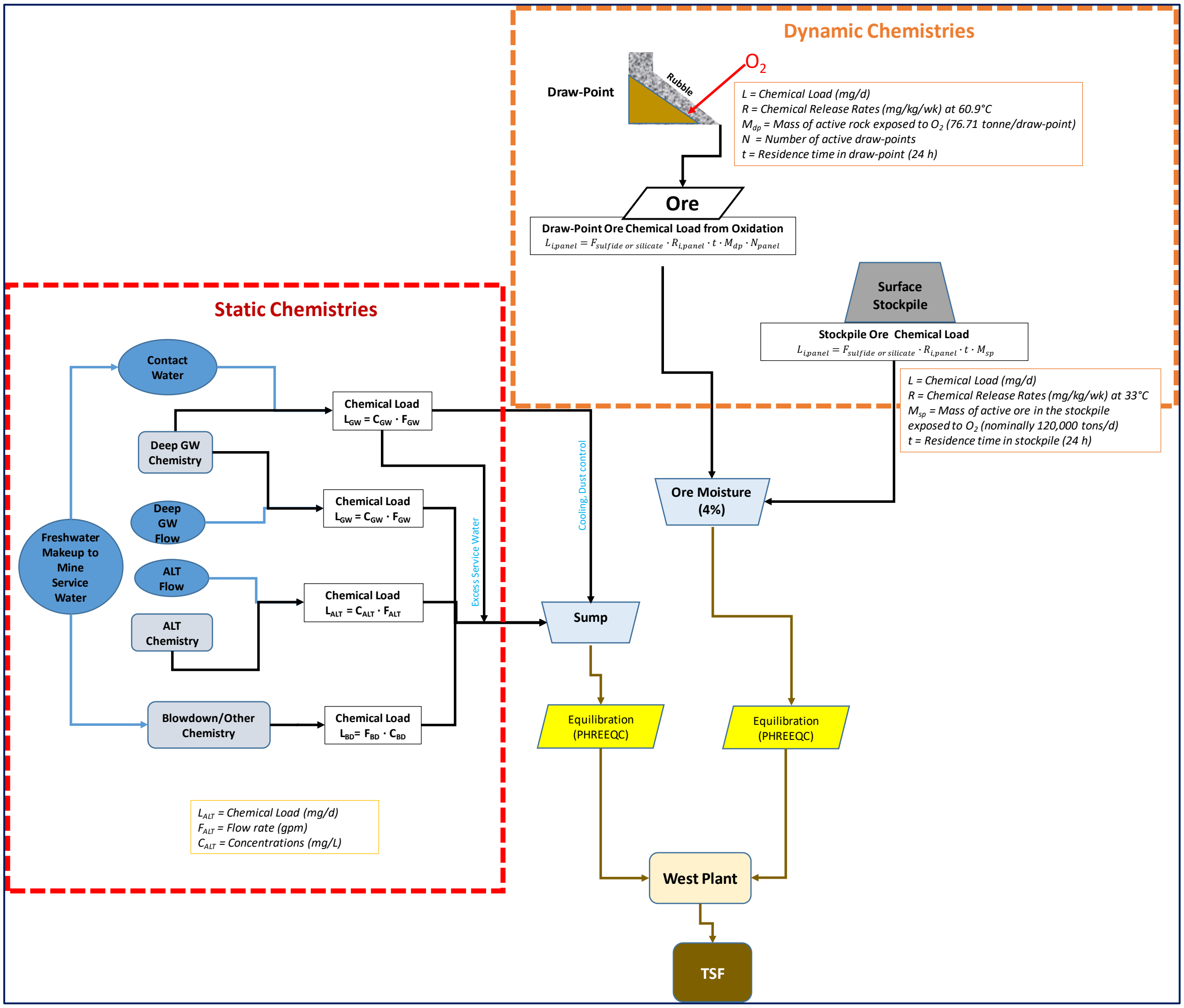

Figure 3-1. Schematic of the calculation logic for the block cave geochemistry model

4 INPUT DATA

4.1 Groundwater Inflow

The model uses inputs for rates of groundwater inflows from the WSP hydrology model (WSP, 2018). Flow rates from this model have been aggregated into two major inflows to the block cave:

- Deep Groundwater – water that flows into the periphery of the block cave and underground levels from the deep groundwater system.
- ALT groundwater – water that is expected to flow into the block through the fracture system created by the block cave.

Figure 4-1 shows the predicted inflow rates from the WSP hydrology model for Deep Groundwater and ALT groundwater. The WSP hydrology model predicts groundwater inflows prior to ore production during development years as well as during the subsequent years of ore production. The flow rates from the WSP model as shown in Figure 4-1 are used directly in the water balance portion of the block cave geochemistry model.

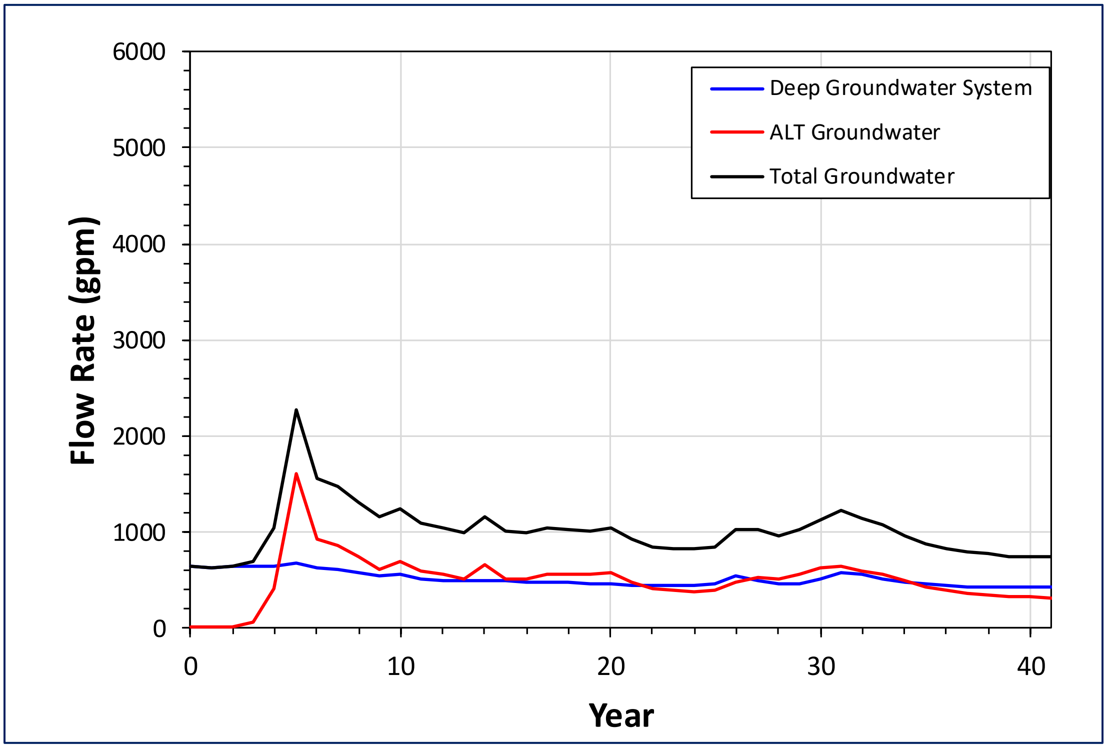

Figure 4-1. Predicted inflow rates to the block cave from the WSP hydrology model.

4.2 Underground Water Balance

A summary of the underground water balance is given in Enchemica (2018). The primary sources of inflow water to the underground will be:

- Groundwater (Figure 4-1)
- Mine Service Water

Mine Service water is comprised of freshwater used for various cooling systems obtained from the Central Arizona Project (CAP) canal and banked Recovery Wells. Figure 4-2 shows predicted rates of water inflows to the underground.

The main water types pumped and conveyed as ore moisture from the underground to the surface for use in the West Plant include:

- Sump (contact) water
- Cooling blowdown water
- Ore Moisture

Figure 4-3 shows predicted rates of water flows from the underground. Sump water includes all water that has been in contact with intact rock within the underground. Cooling blowdown water will likely be combined with sump water but is broken out here because it is expected to carry a relatively high solute load due to evapoconcentration in cooling systems. The rate of water flow as moisture in ore conveyed to the surface is also identified as a separate flow because it is expected to carry a substantial portion of the solute load generated from oxidation and leaching of ore. The difference between the total water inflows and outflows is indicative of the net losses of water to ventilation and cooling systems.

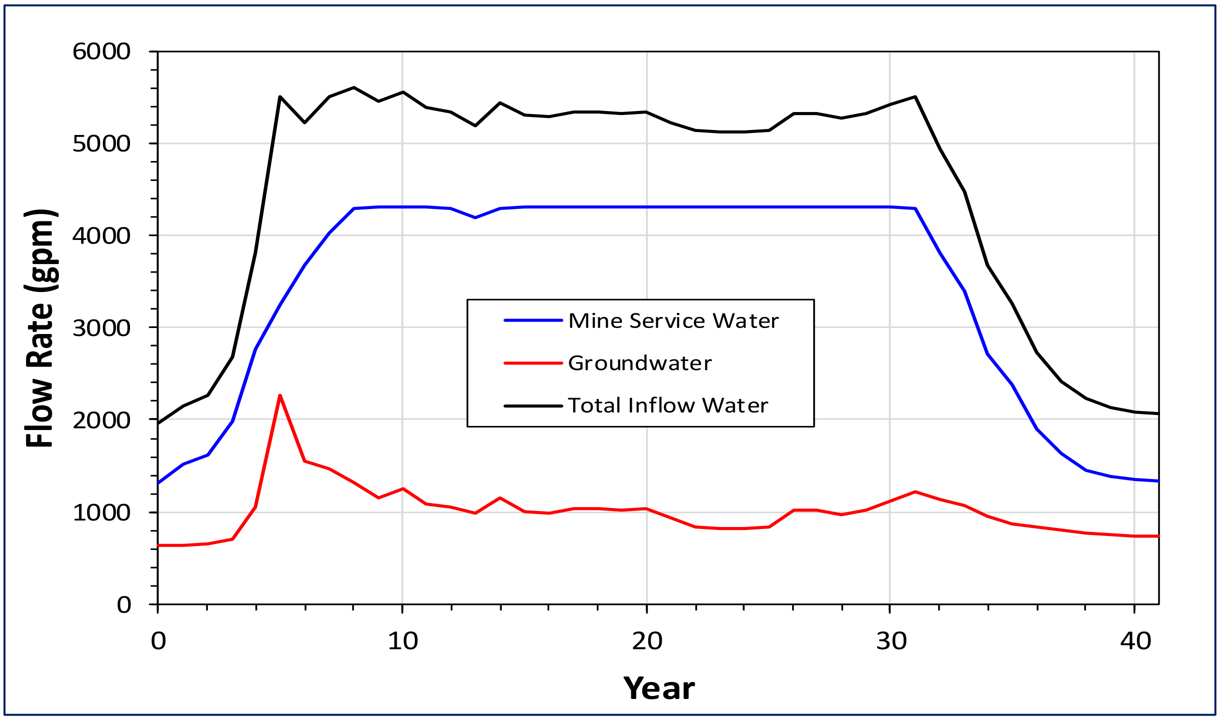

Figure 4-2. Rates of water inflows to the underground

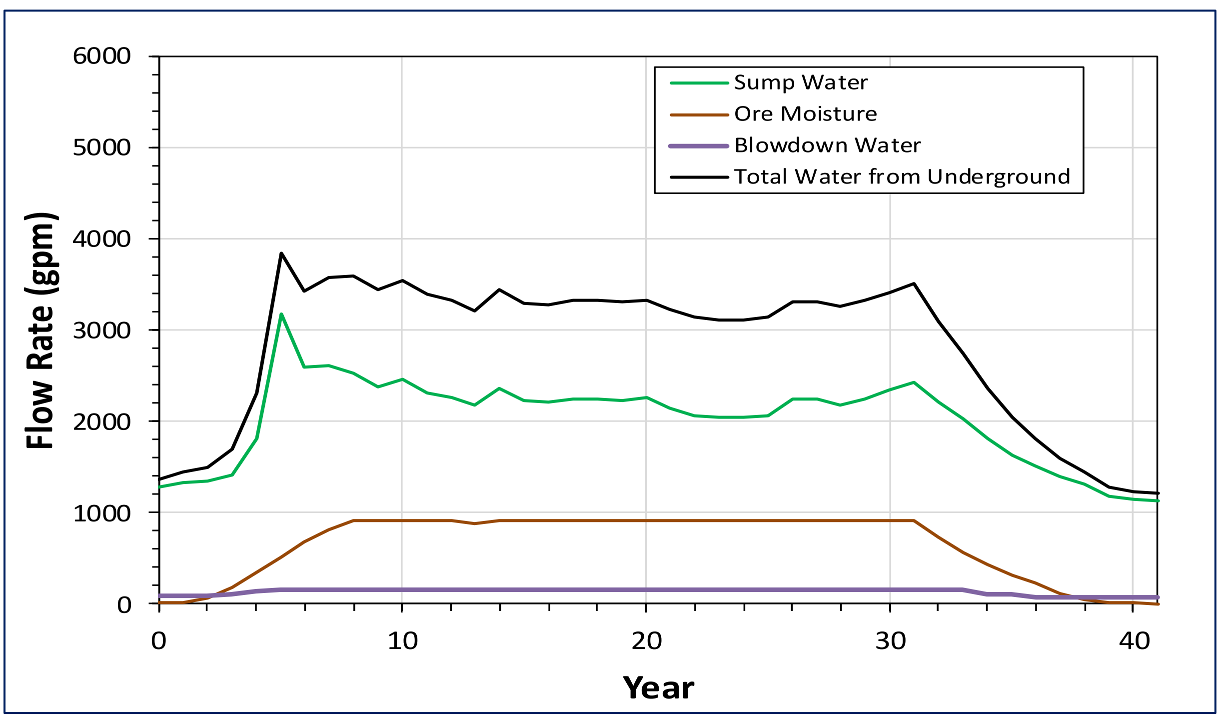

Figure 4-3. Rates of water removal from the underground

4.3 Mining Schedule

4.3.1 Panel Sequence

The model includes the six panels that are outlined in the mine plan. These panels are shown in Figure 4-4 in plan view per the mine plan of operations. Mining will begin at a point far away from Apache Leap in Panel 2 and then progress outward. The expected sequence is Panel 2 followed by Panel 3, Panel 1, Panel 4, Panel 5, and Panel 6 (RC, 2017).

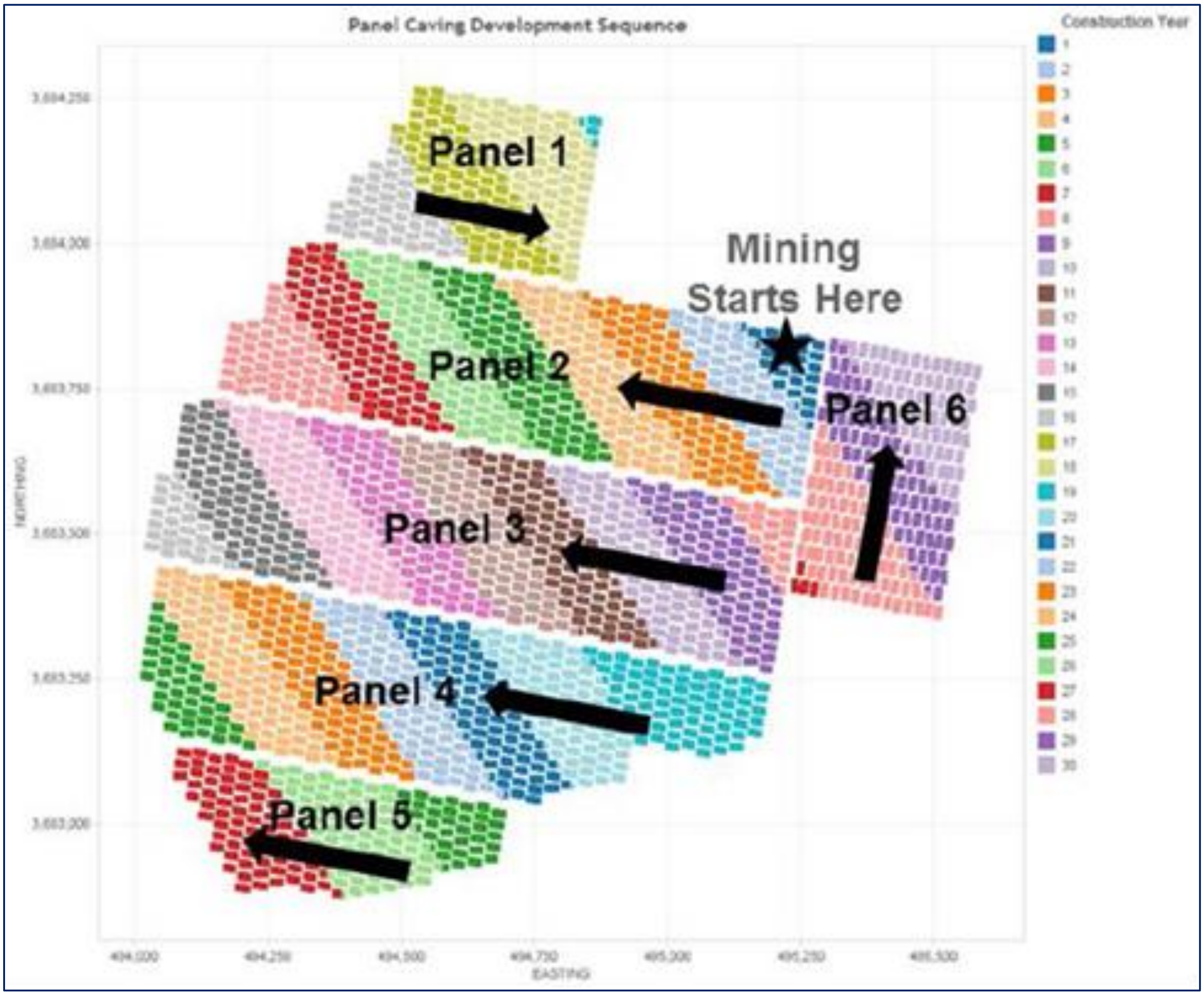

Figure 4-4. Layout of mining panels (RC, 2016)

Figure 4-5 shows the number of active draw-points per panel over time. The total number of active draw-points ranges from about 900 to 1280 during full production. The numbers of active draw-points per panel are tracked and incorporated into the model according to the data in Figure 4-5.

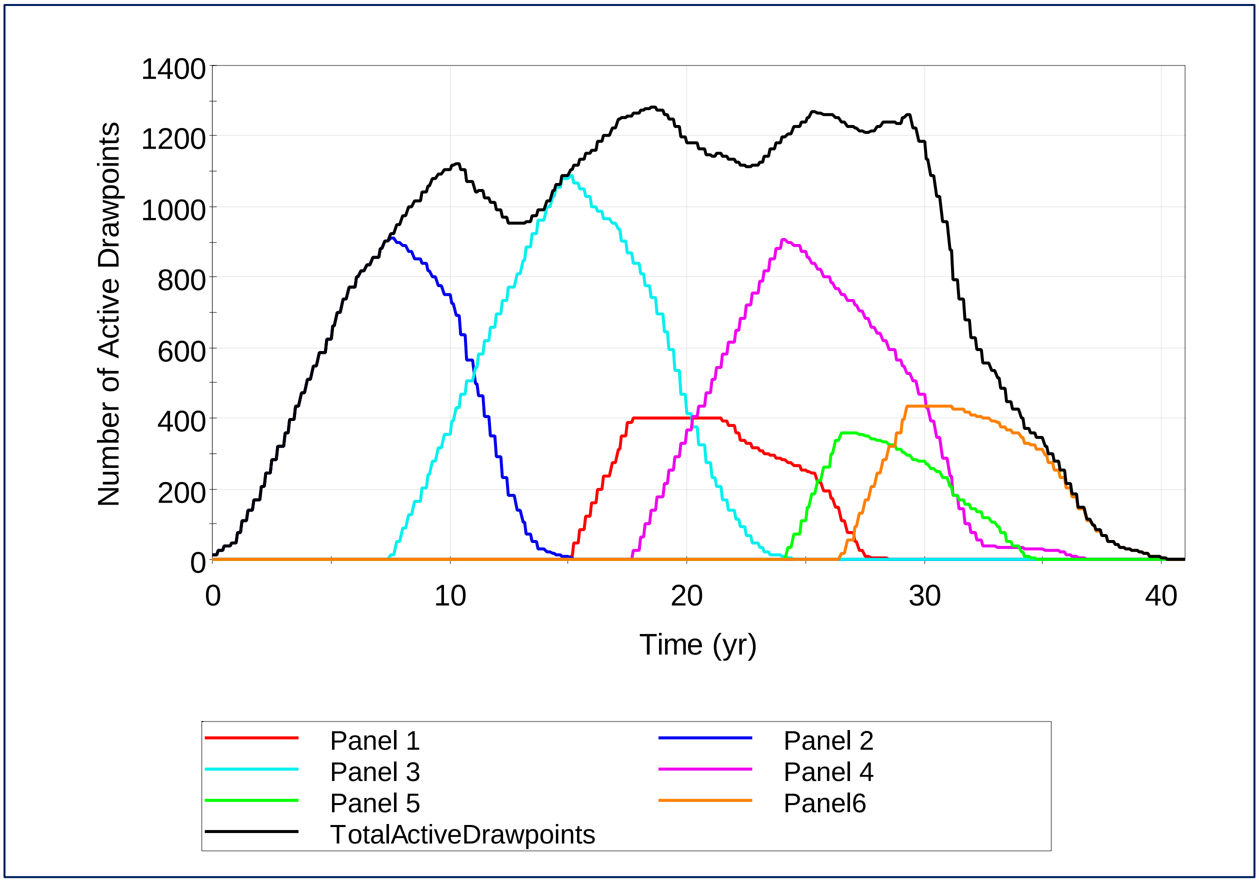

Figure 4-5. Active draw-points per panel over time (RC, 2017)

4.3.2 Ore and Waste Schedule

The schedule for ore and development rock based on the panel sequence and number of active draw-points is shown in Figure 4-6. The estimate of total tonnages are approximately 1.4 billion tons of ore and 33.5 million tons of development rock.

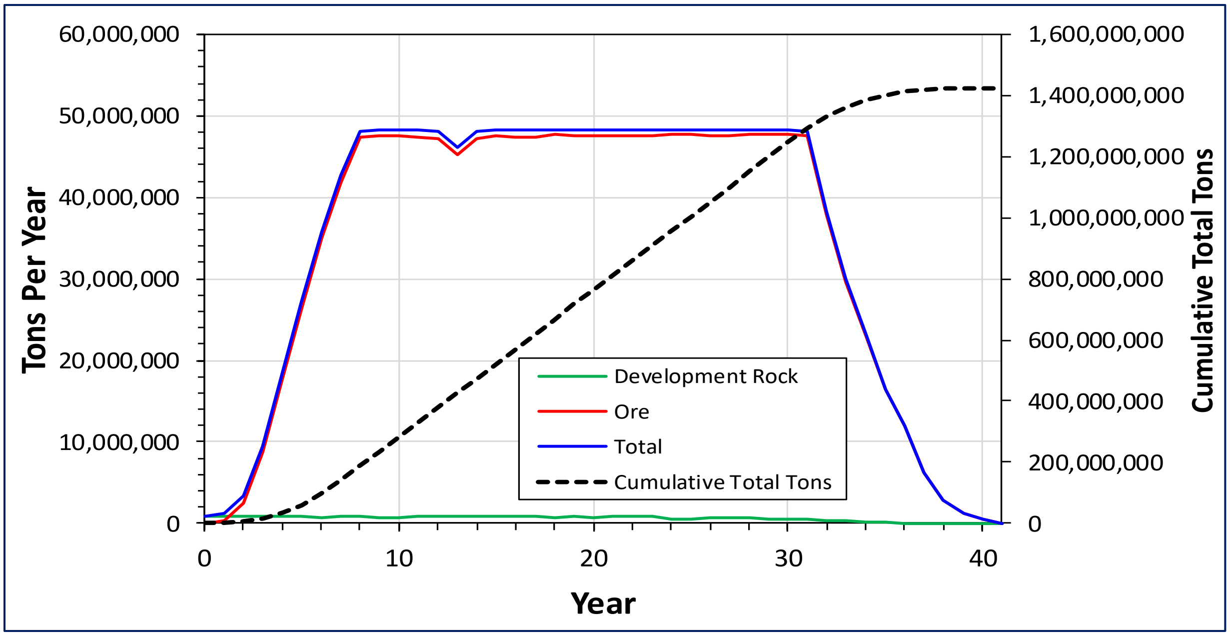

Figure 4-6. Ore and waste schedule (RC, 2016)

4.4 Static Water Chemistries

Static water chemistries refer to chemical compositions for water sources in the underground that are not expected to have substantial changes over time.

4.4.1 Mine Service Water

Mine Service water will be comprised of freshwater makeup obtained from the Central Arizona Project (CAP) canal and banked Recovery Wells. The chemistry of the CAP canal water used in the model is from an analysis of a sample collected in March 2018 (Table 4-1).

The chemical composition for the Recovery Wells in the model is based on data from the 2016 water quality report for Superior, Arizona obtained from the Arizona Water Company (AZ, 2016) (Table 4-1). The report contained concentrations for As, Ba, Cr, Cu, Pb, F, NO_3, Cl, and Na. Concentrations for all other unreported parameters were assumed to be to be same as CAP water.

Based on guidance from RCM, 25% of renewable water will be obtained from the CAP canal and 75% from the Recovery Wells (Table 4-1Table 4-1).

4.4.2 Cooling Blowdown Water

A portion of the mine service water will be used for refrigeration and the cooling system. The blowdown water from these cooling systems will result in return flows to the underground sumps that have undergone some degree of evaporation through use for cooling. It has been assumed that the chemistry of blowdown water can be represented by freshwater that has been evapoconcentrated to a TDS concentration of approximately 2500 mg/L. The evapoconcentration calculation was made with PHREEQC by removing water from the 25% CAP + 75% Recover Well mixture and equilibrating with atmospheric O_2 and CO_2. The resulting chemical composition for blowdown water is given in Table 4-1.

4.4.3 ALT Groundwater

The chemistry of draining into the block cave from the ALT is represented in the model by the average of analyses of samples collected from wells completed in the ALT, including HRES-01, HRES-02, HRES-03, and

HRES-04 (M&A, 2012) (Table 4-2). The average chemistry was calculated using the mixing function in PHREEQC and equilibrating with atmospheric O_2 and specifying a maximum dissolved carbonate content in equilibrium with atmospheric CO_2, assuming they would be in contact with the atmosphere when they reach the block cave.

4.4.4 Deep Groundwater

Water is currently being pumped from the Deep Groundwater system from Shaft 9 and 10. It is assumed that the water in Shaft 9 and 10 is chemically representative of future water that will flow into shafts and ramps around the block cave from the Deep Groundwater system. The chemical composition for Deep Groundwater is also used to represent all Mine Service water that contacts rock surfaces in the underground not including the water comprising ore moisture.

The composition of the Deep Groundwater system was calculated from the average of 22 samples collected from Shaft 9 prior to entering the water treatment plant that is currently in operation. The 22 samples used in the average were collected during the first half of 2015 and are representative of groundwater inflows. Prior to 2015 groundwater inflows were mixed with accumulated water from the Magma Mine underground workings where chemical compositions had fluctuated since 2009 when pump-down of accumulated water in the Magma Mine began. The average water chemistry was calculated using the solution mixing function in PHREEQC with equal mixing proportions for all samples and equilibrating with atmospheric O_2 and specifying a maximum dissolved carbonate content in equilibrium with atmospheric CO_2, assuming they would be in contact with the atmosphere when they reach the block cave. The resulting chemical composition is given in Table 4-2.

Table 4-1. Chemical compositions for CAP Canal and Recovery Well water (mg/L)

Solute	CAP Canal	Recovery Wells	Mixture (25% CAP + 75% Recovery Well)	Blowdown Water
Ca	74	74**	74	357
Mg	26	26**	26	125
Na	94	74	79	381
K	4.9	4.9**	5	24
Cl	98	98**	98	473
Alkalinity	130	130**	130	392
SO_4	250	250**	189‡	914
Si as SiO_2	5.2	5.2**	5.2	25.1
F	0.4†	0.4	0.4	1.9
NO_3-N	0.28	1.4	1.1	5.4
Al	0.013*	0.05	0.04	0.20
Sb	0.00002*	0.00002**	0.00038	0.00184
As	0.002	0.0076	0.06	0.28
Ba	0.13	0.01	0.04	0.19
Be	0.0001*	0.0001**	0.00003	0.0001
B	0.13	0.13**	0.13	0.63
Cd	0.00002*	0.00002**	0.00002	0.00010
Cr	0.00002*	0.004	0.003	0.015
Co	0.00003*	0.00003**	0.0002	0.0009
Cu	0.001	0.05	0.038	0.182
Fe	0.055*	0.055**	0.051	0.247
Pb	0.0011*	0.005	0.004	0.018
Mn	0.0004*	0.0004*	0.004	0.019
Mo	0.0004*	0.0004**	0.004	0.019
Ni	0.00092	0.00092**	0.0009	0.0044
Se	0.0017	0.0017**	0.0017	0.0082
Ag	0.000006*	0.000006**	0.00004	0.0002
Tl	0.0000065*	0.0000065**	0.00004	0.0002
Zn	0.00165*	0.00165**	0.019	0.092
pH (s.u.)	8.5	8.3	8.51	9.07
TDS***	592	530	545	2495

*One-half of the analytical detection level
**Not analyzed, assumed the same as CAP
***TDS = Ca + Mg + Na + K + Cl + SO_4 + 0.4917*HCO_3 + SiO_2 + F + Al + Fe + Mn + Ba + Co + Ni + Cu + Zn (Hem, 1989)
†Not analyzed, assumed the same as Recovery Well water
‡SO4 used to charge-balance solutions

Table 4-2. Water chemistry for the ALT and Deep Groundwater (mg/L)

Solute	ALT Groundwater	Deep Groundwater
Ca	24	307
Mg	4	80
Na	38	142
K	1.5	38
Cl	6.9	22
HCO_3	149	77
SO_4	8.5	1288
Si	61.2	55.5
F	0.40	3.06
NO_3-N	0.97	0.24
Al	0.14	0.054
Sb	0.0148	0.001
As	0.0155	0.0083
Ba	0.0102	0.0267
Be	0.0016	0.0005
B	0.148	0.39
Cd	0.0016	0.0005
Cr	0.0041	0.001
Co	0.0152	0.0033
Cu	0.0076	0.0037
Fe	0.11	0.05
Pb	0.015	0.0005
Mn	0.012	3.6
Mo	0.016	0.012
Ni	0.016	0.0046
Se	0.015	0.001
Ag	0.002	0.005
Tl	0.015	0.0005
Zn	0.028	0.307
pH (s.u.)	8.66	8.15
TDS*	225	1977

*TDS = Ca + Mg + Na + K + Cl + SO_4 + 0.4917*HCO_3 + SiO_2 + F + Al + Fe + Mn + Ba + Co + Ni + Cu + Zn (Hem, 1989)

4.5 Dynamic Water Chemistries

Dynamic water chemistries refer to chemical compositions of water sources that are expected to be functions of time and exposure to sulfide minerals due to oxidation and leaching reactions. A series of calculations are involved in simulating the dynamic water chemistries, including:

- Draw-points
    - Oxidized Ore Mass - Mass of active ore exposed to air in draw-points
    - Residence Time - Length of time for oxidation of active ore in draw-points
    - Solute Release Rates – Oxidation and leaching rates at the elevated temperatures of the draw-points
- Stockpile
    - Oxidized Ore Mass - Mass of ore in the stockpile
    - Residence Time - Length of time for oxidation of ore in the stockpile

- Solute Release Rates - Oxidation and leaching rates at the estimated temperature of the stockpile

An additional set of calculations is used to estimate nitrate release rates because they are assumed to be a result of leaching or blasting residue rather than oxidation and leaching.

4.5.1 Ore Zones

The mass of ore potentially exposed to O_2 and oxidation in draw-points is represented in the model as a function of:

- Mass of active ore at draw-points
- Depth of O_2 penetration into ore at draw-points

The methods used to estimate these parameters are described in the following sections.

4.5.1.1 Mass of Active Ore at Draw-Points

The total mass of active ore is calculated from the product of the number of active draw-points (Figure 4-5) and the mass of active ore per draw-point. The calculation of the mass of active ore per draw-point is based on the expected geometry of an individual draw-point as shown in Figure 4-7. The total exposed area of the active ore in the draw-point face is estimated to be 28.55 m^2 (RC, 2017). The average depth of active ore is estimated to be 1.38 m giving a volume of 39.4 m^3 (RC, 2017). Multiplication of the draw-point dimensions and bulk density of 1.6 tonne/m^3 (RC, 2017) yields a mass of 63.04 tonne (69.49 ton) of active ore in the face of the draw-point. The potential also exists for O_2 to penetrate the top of a draw-point to a depth of 1.38 m, yielding an additional 8.57 m^3 or 13.71 tonne (15.11 ton) of potentially oxidized ore. The total for the face and top of a draw-point is 76.71 tonne (84.56 ton). Multiplication of 76.71 tonne per draw-point by the number of active draw-points yields the mass of sulfide ore exposed to O_2 at any given time (Figure 4-8). The GoldSim model tracks the total mass of active ore over time based on this approach. The model also includes the schedule for closing of draw-points and panels over time as the ore is depleted. Ventilation would cease after panels are closed and as such, oxidation would also cease and no longer produce a solute load due to oxidation to in the block cave.

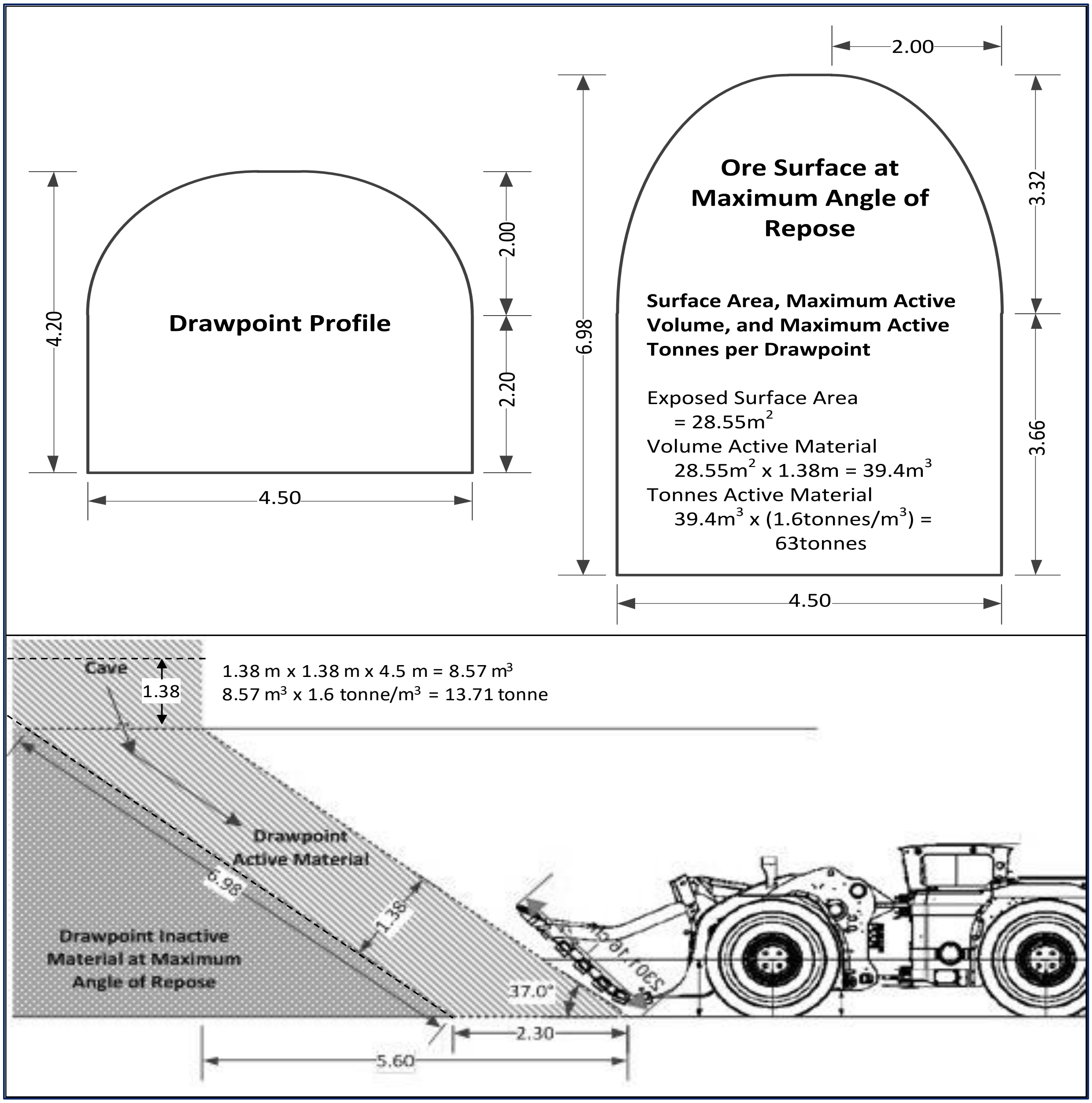

Figure 4-7. Geometry of an individual draw-point (RC, 2017)

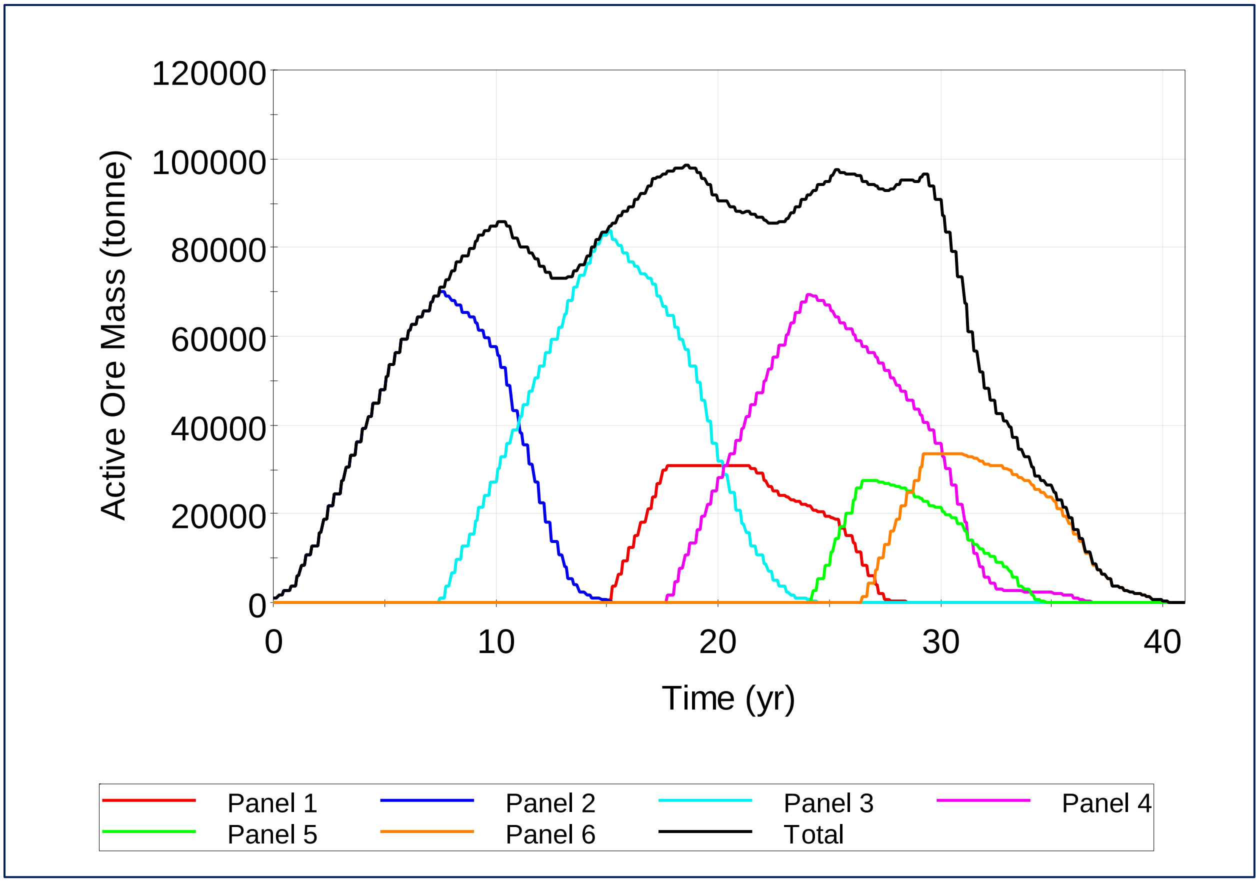

Figure 4-8. Ore mass exposed to oxidation per panel over time

4.5.1.2 Oxidation Zone Thickness

The thickness of the oxidation zone for ore in draw-points was calculated with an associated model that is described in Enchemica (2018b). Based on the results of that model, it has been assumed that the entire thickness of the active ore of 1.38 m is potentially exposed to O_2. The rates solute release resulting from sulfide oxidation and silicate dissolution are calculated as functions of the temperature of the rock in the draw-points, accounting for the depletion of O_2 with depth into the active ore as O_2 is depleted by sulfide oxidation. The solute release rates are discussed below in Section 4.5.1.4.

4.5.1.3 Residence Time of Active Ore

The draw-points are the locations where ore will be continuously moving downward to extraction levels. The residence time refers to the time that ore physically resides in a draw-point before being removed by loaders and placed on conveyors. The residence time is used here for calculating the reaction time for sulfide oxidation and associated solute release rates.

The residence time of ore in the draw-points was examined in a simulation study of mine production by Labrecque (2017). Figure 4-9 shows results from that study for simulations at peak production. The results indicate that active ore in draw-points will have an average residence time of about 24 h.

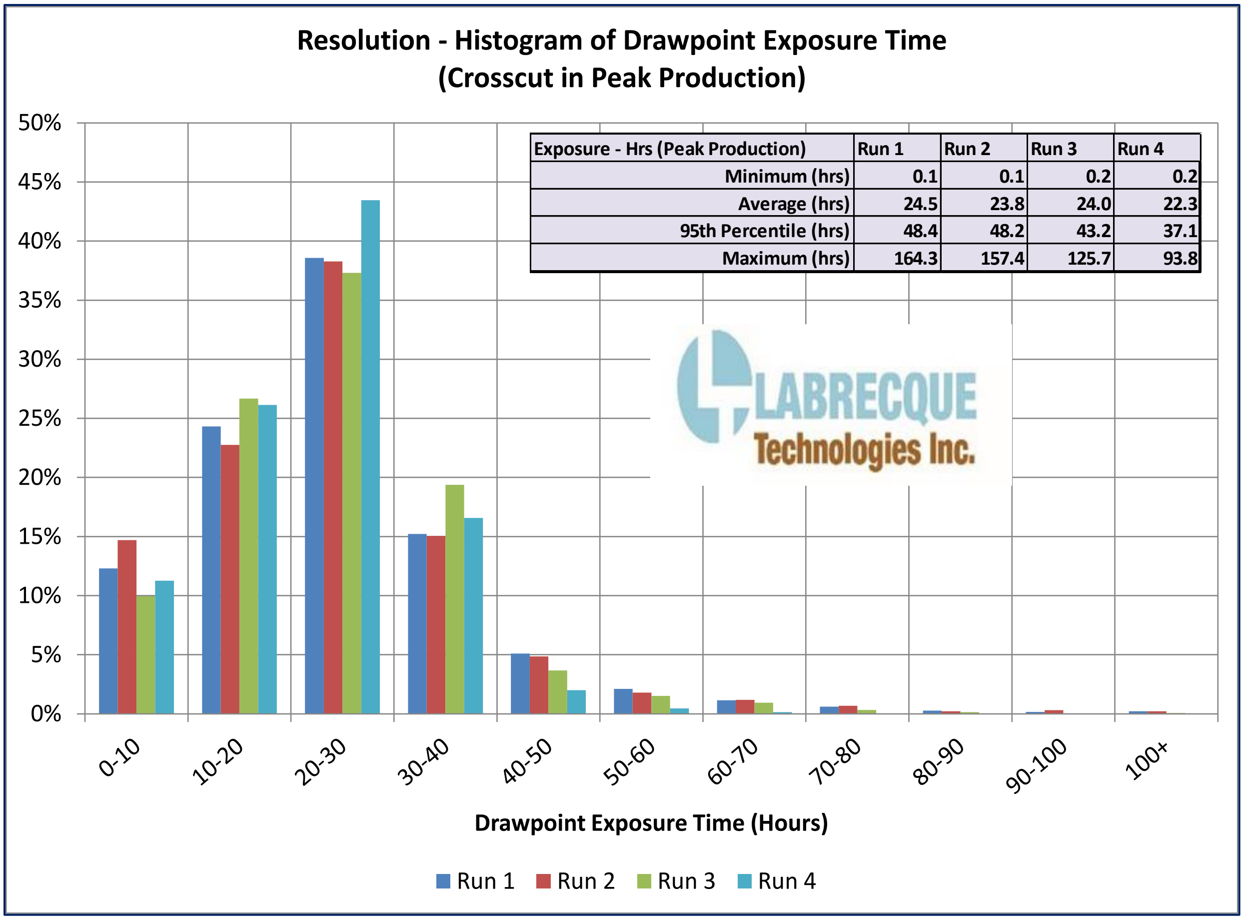

Figure 4-9. Histogram of ore residence time in draw-points

4.5.1.4 Solute Release Rates

Release rates in mg/kg/wk for all solutes were calculated from concentrations measured during the last three weeks of laboratory kinetic tests divided by the sample weight (MWH, 2013). The release rates are assumed to be representative of fully oxidized and approximate steady-state conditions achieved in many of the kinetic tests.

Table 4-3 gives a summary of the samples used in the kinetic tests. Kinetic tests conducted on samples with less than 0.5% sulfide-S were not used in rate calculations because it was assumed these samples were outside of ore zones and would not be exposed to O_2 at draw-points. Many of the kinetic test samples with more than 0.5% sulfide-S were found to be outside the panel boundaries upon review of the geologic model. The kinetic test data for these samples were retained in the release rate calculations because their sulfide contents and drill-hole depths are expected to be representative of ore zones.

The kinetic tests were conducted on the range of lithologies and alteration types expected to exist in the block cave (

Table 4-3). The approach used to aggregate the kinetic leaching data for use in the model was:

- The kinetic data were grouped by lithology:
    - Dm+Skn: Martin limestone and skarn
    - Diab: Diabase
    - Kvs: Cretaceous volcanics and undifferentiated sediments
    - QEP: Quartz eye porphyry

- Qzite: Quartzite
- Average release rates were calculated for each of the above five main lithologic types
- The geologic model of the deposit was used to obtain the masses of each lithology predicted to exist in each panel (Table 4-4). The block model lithologies were aggregated into the five lithologies identified for the kinetic tests in MWH (2013) with assistance from the Resolution geologists. The aggregations are given in Table 4-5.
- The masses of each lithology in the panels were converted to percentages. These percentages were applied to the average release rates calculated for each of the five lithologies to give weighted average release rates for each panel (Table 4-6).

Table 4-3. Summary of kinetic tests from MWH (2013) (samples in gray not used for release rates)

Sample ID	Lithology	Alteration	HCT Test ID	Panel	Sulfide-S (%)
RES-008A 1597-1600	Kvs	HFL	33	outside	0.0096
RES-005I 1317.28-1320.28	Tw	UNALT	15	outside	0.032
RES-005I 1428.18-1431.18	Kvs	AA	16, 16S, 17, 17S	outside	0.032
RES-005I 1586.46-1589.46	QEP	PHY	19, 19S	outside	0.032
RES-009 278.9-281.09	Tal	UNALT	38	outside	0.032
RES-009 645.59-647.52	Tw	UNALT	39	outside	0.032
RES-009 804.84-807.00	Tw	UNALT	40, 41	outside	0.032
RES-009 994.67-997.67	Kvs	SA	42	outside	0.032
RES-002A 888-891	Kvs	PHY	9, 9S	outside	0.064
RES-005I 1499-1502	Kvs	PHY	18, 18S	outside	0.064
RES-001C 1771.75-1791.4	Dm	SKRET	3	outside	0.576
RES-001C 1855-1858	Dm	SKRET	4, 4S, 5	outside	0.832
RES-001C 1745-1748	Kvs	POT	2	outside	1.088
RES-001C 1639-1642	Kvs	PRO	1	outside	1.664
RES-006D 1952.56-1954.83	Qzite	PHY	29, 29S	outside	1.728
RES-001C 1873-1876	Dm	HFLRET	6	outside	2.176
RES-009E 2056.38-2075	Diab	POT	54	outside (below)	2.176
RES-009E 1739.63-1742.63	Qzite	AA	49, 49S	outside	2.432
RES-009E 1984.74-1987.74	Qzite	POT	53	2	2.432
RES-006D 2091.13-2094.13	Diab	POT	32, 32S	1	2.528
RES-002A 1927-1930	Diab	POT	14	4	2.592
RES-005I 1892.81-1895	Qzite	PHY	24	3	2.816
RES-002A 1154-1156	Kvs	PHY	10, 10S	outside	2.912
RES-006D 1954.83-1972	Qzite	ZEO	30	outside	3.168
RES-005I 1917.29-1919.1	Diab	POT	25, 25S	3	3.52
RES-001C 2041-2044	Diab	POT	7, 8	outside	3.584
RES-005I 1632.56-1635.56	Kvs	PHY	20, 20S	outside	4.192
RES-008A 1717-1720	Kvs	PRO	34	outside	4.32
RES-005I 1652-1654.93	QEP	PHY	21	outside	4.672
RES-009E 1351.03-1354.03	Kvs	PHY	43	outside	4.832
RES-005I 1759.23-1761.23	QEP	PHY	23	3	4.864
RES-005J 1660.4-1668.47	QEP	PHY	26	6	5.184
RES-006D 1898.21-1901.09	Qzite	PHY	28	outside	5.632
RES-005I 1654.93-1657.3	QEP	PHY	22, 22S	outside	5.696
RES-002A 1414.6-1417	QEP	PHY	11	outside	6.56
RES-009E 1899-1901.88	Dm	SKRET	52, 52S	2	6.88
RES-009E 1634.46-1637.47	Kvs	PHY	48, 48S	outside	6.976
RES-009E 1867.87-1884.35	Dm	SKRET	51	2	7.264
RES-009E 1829.95-1832.48	Dm	SKRET	50	2	7.68
RES-002A 1454-1457	Kvs	PHY	12, 13	outside	8.8
RES-008A 1844.1-1846.6	Skn	PHY	35	outside	9.84
RES-009E 1510.74-1527.19	Kvs	PHY	44, 45, 46	outside	9.888
RES-006D 1750.4-1753.4	Kvs	PHY	27	outside	10.592
RES-008A 2053.81-2056.81	Diab	PHY	37	outside (below)	11.9008
RES-006D 1980.6-1983.6	Qzite	PHY	31, 31S	outside	12.704

RES-009E 1597.32-1599.88	Kvs	PHY	47, 47S	outside	14.496
RES-008A 1979.95-1982.94	Qzite	SIL	36	outside	22.3008

Table 4-4. Masses and percentages of lithologies per panel

	Amount	Kvs	QEP	Diabase	Dm+Skn	Qzite	Totals*
Panel 1	short tons	20,915,993	5,060,391	77,400,292	13,985,428	46,667,350	164,029,453
	Percentage	12.75%	3.09%	47.19%	8.53%	28.45%	100.00%
Panel 2	short tons	35,499,334	18,475,672	243,568,516	35,416,140	78,140,993	411,100,655
	Percentage	8.64%	4.49%	59.25%	8.61%	19.01%	100.00%
Panel 3	short tons	66,673,320	106,350,601	187,890,249	38,762,395	73,139,948	472,816,513
	Percentage	14.10%	22.49%	39.74%	8.20%	15.47%	100.00%
Panel 4	short tons	27,570,098	25,149,666	253,734,229	23,604,103	53,740,298	383,798,394
	Percentage	7.18%	6.55%	66.11%	6.15%	14.00%	100.00%
Panel 5	short tons	1,357,211	543,744	73,125,950	3,321,183	16,412,998	94,761,086
	Percentage	1.43%	0.57%	77.17%	3.50%	17.32%	100.00%
Panel 6	short tons	0	79,328,170	42,983,600	208,836	308,672	122,829,277
	Percentage	0.00%	64.58%	34.99%	0.17%	0.25%	100.00%

*Total panel tons include the entire dimensions of panels including non-ore portions so exceeds planned total ore production (Figure 4-6).

Table 4-5. Aggregation of lithologies and definitions

HCT Lithology		Geologic Model Lithology
Dm+Skn	=	mescr+pzlssr+mescd+pzlssd+bx3
Diabase	=	diab+bx+basalt
Kvs	=	Kvs
QEP	=	QEP
Qzite	=	Kqs+qzite1+qzite2+qzite3+azite3a+qzite4

Abbreviation	Definition
Dm	Devonian Martin Limestone
Diab, Diabase	Diabase
Kvs	Cretaceous volcanics and undifferentiated sediments
QEP	Quartz eye porphry
Qzite	Quartzite
mescr, pzalssr	Mescal and Paleozoic retrograde skarns
Mecsd, pzlssd	Skarn destructive (former retrograde skarn with little or no Ca remaining)
bx	Breccia (mostly diabase)
Kqs	Cretaceceous quartz rich sediments
Basalt	Basalt

Table 4-6. Release rates from the kinetic tests weighted by lithology per panel at 25°C

	mg/kg/wk					
Solute	**Panel 1**	**Panel 2**	**Panel 3**	**Panel 4**	**Panel 5**	**Panel 6**
Ca	30.2024	30.3873	23.5478	30.3270	33.6021	12.6832
Mg	0.5550	0.6245	0.5133	0.6344	0.6661	0.4091
Na	0.3720	0.3758	0.3819	0.3719	0.3683	0.4090
K	1.0655	1.1818	1.0400	1.2360	1.2972	0.9923
Cl	0.8578	0.8813	0.8546	0.8996	0.9206	0.8757
HCO_3	3.2185	3.3649	3.0158	3.3232	3.2714	1.9446
SO_4	84.6787	82.8030	76.4064	82.0023	86.4938	68.4279
Si	2.0356	1.8430	2.3357	1.7615	1.5728	2.9974
F	0.9530	0.7913	0.7405	0.6874	0.7231	0.4619
NO_3-N*	0.0000	0.0000	0.0000	0.0000	0.0000	0.0000
Al	0.5847	0.5111	0.9049	0.4931	0.3647	1.6692
Sb	0.00032	0.00031	0.00034	0.00031	0.00031	0.00039
As	0.00043	0.00046	0.00085	0.00050	0.00037	0.00178
Ba	0.00479	0.00495	0.00594	0.00513	0.00486	0.00864
Be	0.00167	0.00163	0.00177	0.00161	0.00157	0.00200
B	0.00850	0.00824	0.00890	0.00818	0.00796	0.00985
Cd	0.00152	0.00111	0.00119	0.00090	0.00097	0.00101
Cr	0.00807	0.00797	0.00884	0.00800	0.00771	0.01051
Co	0.01402	0.01224	0.01419	0.01142	0.01103	0.01653
Cu	7.7832	6.4481	11.6627	6.0084	4.3282	21.2611
Fe	0.7383	0.6409	1.6985	0.6730	0.2870	3.6786
Pb	0.00373	0.00252	0.00209	0.00189	0.00230	0.00019
Mn	0.1357	0.1487	0.1102	0.1551	0.1756	0.0785
Mo	0.00798	0.00798	0.00856	0.00802	0.00787	0.01002
Ni	0.01351	0.01239	0.01394	0.01192	0.01170	0.01673
Se	0.00494	0.00601	0.02185	0.00767	0.00242	0.05875
Ag	0.00506	0.00498	0.00547	0.00500	0.00487	0.00651
Tl	0.00008	0.00008	0.00009	0.00008	0.00008	0.00011
Zn	0.4673	0.3273	0.3120	0.2551	0.2725	0.0800

*NO_3-N release rates were estimated from blasting use (see below)

4.5.1.5 Temperature Effects on Reaction Rates

The release rates in Table 4-6 are derived from laboratory tests conducted at 25°C. The active ore in draw-points is expected to have higher temperatures, ranging up 74°C (Moreby, 2018). Figure 4-10 shows the temperature profile for draw-points for a 24-h residence time from Moreby (2018). In addition, as O_2 moves into ore, it will be consumed resulting in decreased rate of sulfide mineral oxidation. The increase in temperature will increase reaction rates with depth into the ore, whereas the decrease in O_2 will decrease sulfide oxidation rates. These two effects were accounted for by incrementally adding their combined effects over 0.1-m intervals up to a depth of 1.4 m (rounding up from 1.38 m for the active ore zone, Figure 4-7), which covers the entirety of the thickness of the oxidation zone in active ore at draw-points (Enchemica, 2018b). In this calculation, which is described below, the O_2 levels at each 0.1-m interval were obtained by the model of oxidation zone thickness (Enchemica, 2018b). The temperatures at each 0.1-m interval are from Moreby (2018).

The effects of temperature and O_2 on sulfide mineral oxidation for each 0.1-m depth interval are based on the activation energy of 56.9 kJ/mol and 0.5-order dependence on O_2 for pyrite from McKibben and Barnes (1986). The use of this activation energy and O_2 dependence from McKibben and Barnes (1986) assumes that O_2 is the primary oxidant for sulfide minerals at draw-points because the 24-h residence time is expected to be too short for ferric ion to become a primary oxidant.

A similar approach was applied to account for the effects of temperature on silicate dissolution based on an activation energy of 29 kJ/mol for phlogopite and pyrophyllite (Palandri and Kharaka, 2004). These two silicates have limited reactivity except at low pH, but are potential sources of some elements (e.g., Al, B, Na, K) typically found in silicate minerals rather than sulfides.

In the model, the temperature factors are applied to calculate mass loads of each solute *i* released ($L_{i,panel}$) in mg) as:

$$L_{i,panel} = F_{sulfide\ or\ silicate} \cdot R_{i,panel} \cdot t \cdot M_{dp} \cdot N_{panel} \qquad \text{Eq. 1}$$

where $F_{sulfide\ or\ silicate}$ is the combined temperature and O_2 factor for either sulfide oxidation or silicate dissolution, $R_{i,panel}$ is the release rate for each solute *i* in mg/kg/wk specific to each panel at 25°C (Table 4-6), t is the residence time (24 h), M_{dp} is the mass of active ore in each draw-point (76.71 tonne), and N_{panel} is the number of active draw-points.

In Eq. 1, $F_{sulfide}$ is defined as:

$$F_{sulfide} = F_T \cdot F_{O_2} \cdot 0.071 \qquad \text{Eq. 2}$$

for a single 0.1-m depth interval, where F_T and F_{O2} refer to the individual temperature and O_2 factors and 0.071 refers to the fraction of a single 0.1-m depth interval relative to the total oxidation thickness depth of 1.4 m. The total for the entire 1.4-m depth is obtained by summing $F_{sulfide}$ from the 0.1-m depth intervals.

A similar approach was used for silicate temperature factor except there is no additional O_2 effect such that:

$$F_{silcate} = F_T \cdot 0.071 \qquad \text{Eq. 3}$$

Table 4-7 gives a summary of the calculations: the depth-weighted average temperature is 60.9°C, $F_{sulfide}$ = 5.04, and $F_{silicate}$ = 3.74.

Table 4-8 summarizes how the temperature factors that were applied to the release rates for individual solutes to account for the combined effects of temperature and O_2 availability. Solutes expected to be associated with sulfide minerals were assigned the temperature factor of 5.04 calculated for sulfide mineral oxidation. Solutes expected to be associated with silicates were assigned the temperature factor of 3.74 calculated for silicate mineral dissolution.

Table 4-7. Summary of temperature and O_2 factors used for solute release rates

			Sulfide Oxidation			Silicate Dissolution	
Depth into Draw-Point (m)	Fraction of 1.4 m	24-h Temp-erature (°C)	F_T	F_{O2}	$F_{sulfide} = F_T \cdot F_{O2} \cdot 0.071$	F_T	$F_{silicates} = F_T \cdot 0.071$
0.1	0.071	33	1.823	1.000	0.130	1.358	0.097
0.2	0.071	40	3.006	0.873	0.188	1.752	0.125
0.3	0.071	46	4.535	0.763	0.247	2.161	0.154
0.4	0.071	52	6.739	0.666	0.321	2.644	0.189
0.5	0.071	57	9.271	0.582	0.385	3.111	0.222
0.6	0.071	61	11.885	0.508	0.431	3.531	0.252
0.7	0.071	65	15.146	0.444	0.480	3.995	0.285
0.8	0.071	67	17.062	0.388	0.472	4.245	0.303
0.9	0.071	69	19.193	0.339	0.464	4.508	0.322
1	0.071	71	21.561	0.296	0.455	4.783	0.342
1.1	0.071	72	22.841	0.258	0.421	4.926	0.352
1.2	0.071	73	24.189	0.226	0.390	5.072	0.362
1.3	0.071	73	24.189	0.197	0.340	5.072	0.362
1.4	0.071	74	25.607	0.172	0.315	5.222	0.373
				Totals=	**5.04**		**3.74**

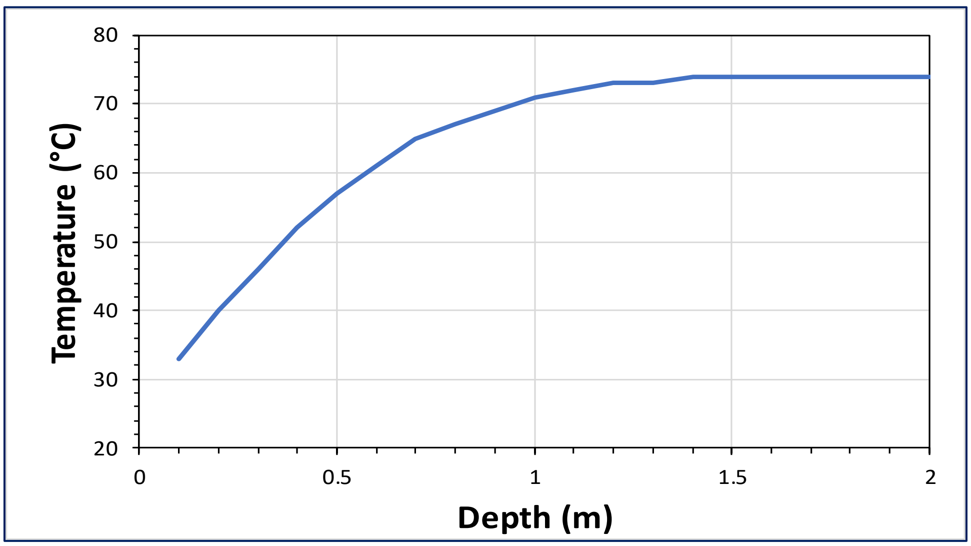

Figure 4-10. Temperature profile for ore in draw-points for 24 h period (Moreby, 2018)

Table 4-8. Temperature factors ($L_{i,panel}$) applied to solute release rates from Table 4-6

Solute	Draw-Points	Stockpile
Ca	3.74	1.358
Mg	3.74	1.358
Na	3.74	1.358
K	3.74	1.358
Cl	3.74	1.358
HCO_3	3.74	1.358
SO_4	5.04	1.823
SiO_2	3.74	1.358
F	3.74	1.358
NO_3	1	1
Al	3.74	1.358
Sb	5.04	1.823
As	5.04	1.823
Ba	5.04	1.823
Be	3.74	1.358
B	3.74	1.358
Cd	5.04	1.823
Cr	5.04	1.823
Co	5.04	1.823
Cu	5.04	1.823
Fe	5.04	1.823
Pb	5.04	1.823
Mn	5.04	1.823
Mo	5.04	1.823
Ni	5.04	1.823
Se	5.04	1.823
Ag	5.04	1.823
Tl	5.04	1.823
Zn	5.04	1.823

4.5.2 Ore Stockpile

The model includes solute releases resulting from storage of ore in the surface stockpile. The approach used to calculate solute releases is similar to that described above for draw-points but with a few simplifications:

- Residence time for ore in the stockpile is assumed to be the same as for active ore zones at 24 h.
- All the ore delivered in 24 h according to the ore schedule is in contact with atmospheric O_2.
- The temperature is assumed to be 33°C, which is the temperature at the surface of ore in draw-points (Moreby, 2018).
- The temperature is the only factor applied to the release rates, assuming the ore placed in the stockpile over a 24-h period is completely exposed to atmospheric O_2.

The factors applied to solute release rates for the stockpile are given in Table 4-8.

4.6 Nitrate

The model has an estimated release rate of NO_3-N based on the expected rate of explosives use of 1 x 10^6 kg per year at full production of 120,000 tonne/d. This rate is equivalent to 0.0069 kg NO_3-N/tonne, assuming a N content of 35% in ANFO (as NH_4NO_3), an ANFO content of 85% in an emulsion/ANFO mixture, and all residual N becomes NO_3. In addition, it is assumed that 5% of this total NO_3-N is readily leachable (Ferguson and Leask, 1988; Bailey et al. 2011).

5 SOLUBILITY EQUILIBRIA

Solution mixtures are equilibrated with the solubilities of secondary minerals at two locations in the model:

- Sump water – mixing of all water types in the mine sump
- Ore moisture – solute releases from oxidation and leaching of ore in draw-points and stockpile and mixing into ore moisture

The PHREEQC geochemical model was used for solution equilibria calculations (Parkhurst and Appelo, 2013). Table 5-1 gives a summary of the parameters used to specify equilibrium conditions with PHREEQC for the sump water and ore moisture.

Table 5-1. Parameters used for equilibrium chemical processes simulated with PHREEQC

Parameter	Value
Temperature	33°C
Partial pressure O_2(g) Partial pressure CO_2(g)	$10^{-0.7}$ atm $10^{-3.5}$ atm
Secondary minerals specified as solubility controls (Only allowed to precipitate if oversaturation conditions exist)	Anglesite, $PbSO_4$ Anhydrite, $CaSO_4$ Antlerite, $Cu_3(OH)_4SO_4$ $Al(OH)_3$(am) Barite, $BaSO_4$ $Be(OH)_2$(am) Brochantite. $Cu_4(OH)_6SO_4$ Chalcedony, SiO_2 Spertiniite, $Cu(OH)_2$ Ferrihydrite, $Fe(OH)_{3(a)}$ Fluorite, CaF_2 Manganite, MnOOH Zincite, ZnO(a) Zincosite, $ZnSO_4$
Adsorption/Desorption	Surface Adsorption (mass determined from simulated amount of $Fe(OH)_3$(a) precipitated per time step; surface area equal to 600 m^2/g; molecular weight of 89 g/mol) Hfo_wOH = 0.2 mol/mol Fe (weak) Hfo_sOH = 0.005 mol/mol Fe (strong)

6 WATER CHEMISTRY PREDICTIONS

Predictions of water chemistry for the sump water and ore moisture are given in Table 6-1 and Table 6-2, respectively. The concentrations in these table are annual averages over the 41-year simulation period.

Predictions of concentration time histories are also shown in Figure 6-1 and Figure 6-3. These time histories show the following characteristics:

- Figure 6-1a and b: The sump water is predicted to be slightly alkaline in pH with TDS concentrations typically around 1500 mg/L. The ore moisture is predicted to be acidic with pH from about 2.3 to 3.5 and have TDS concentrations typically around 4500 mg/L.
- Figure 6-1c and d: Sulfate is the major anion in both sump water and ore moisture. Sulfate concentrations in sump water are predicted to about 1000 mg/L compared to about 3000 mg/L for ore moisture. Bicarbonate and Cl have the next highest concentrations in sump water at concentrations of about 50 and 110 mg/L, respectively. The ore moisture has no HCO_3 due to the low pH such that Cl and F are predicted to have the next highest concentrations at about 30 mg/L for both.
- Figure 6-2a and b: Calcium is the predominant cation for both sump water and ore moisture. Magnesium and sodium are predicted to be at higher concentrations in sump water than ore moisture. This result is due to the addition cooling blowdown water, which has elevated concentrations of these cations due to evaporation, into the sump water.
- Figure 6-2c and d: Concentrations of Al, Fe, and Mn are predicted to be low in the sump water due to the alkaline pH. Concentrations in the ore moisture are predicted to be much higher because of the low pH.
- Figure 6-3a and b: The predicted concentrations of divalent metals follow the same trends as Al, Fe, and Fe. Concentrations are predicted to be low in the sump water with Zn highest at about 0.2 mg/L. In comparison, the concentrations of all metals predicted to be elevated in the ore moisture with Cu the highest at 400 to 500 mg/L followed Zn at 10 to 20 mg/L. Other metals are predicted to occur at much lower concentrations in ore moisture.
- Figure 6-3c and d: The same trends occur for the anionic metals and metalloids. Concentrations in the sump water are predicted to be low with As highest at about 0.02 mg/L. Concentrations in the ore moisture are predicted to be higher with Se highest at about 1 mg/L followed by Mo at about 0.4 mg/L.

The predictions of acidic compositions with higher concentrations of most solutes for ore moisture compared to sump water are due to the assumption that the products of sulfide oxidation and metal leaching will be produced primarily at the draw-points where ore is exposed to O_2 at elevated temperatures and that those products will be transported to the mill in the moisture content of the ore. In comparison, the sump water is comprised of a mixture of groundwater, mine service water, and cooling blowdown water. These water types are neutral to alkaline with comparatively much lower TDS and metal concentrations. The cooling blowdown water brings higher TDS concentrations to this mixture such that the sump water while predicted to be alkaline with some elevated concentrations of SO_4, Ca, and Na.

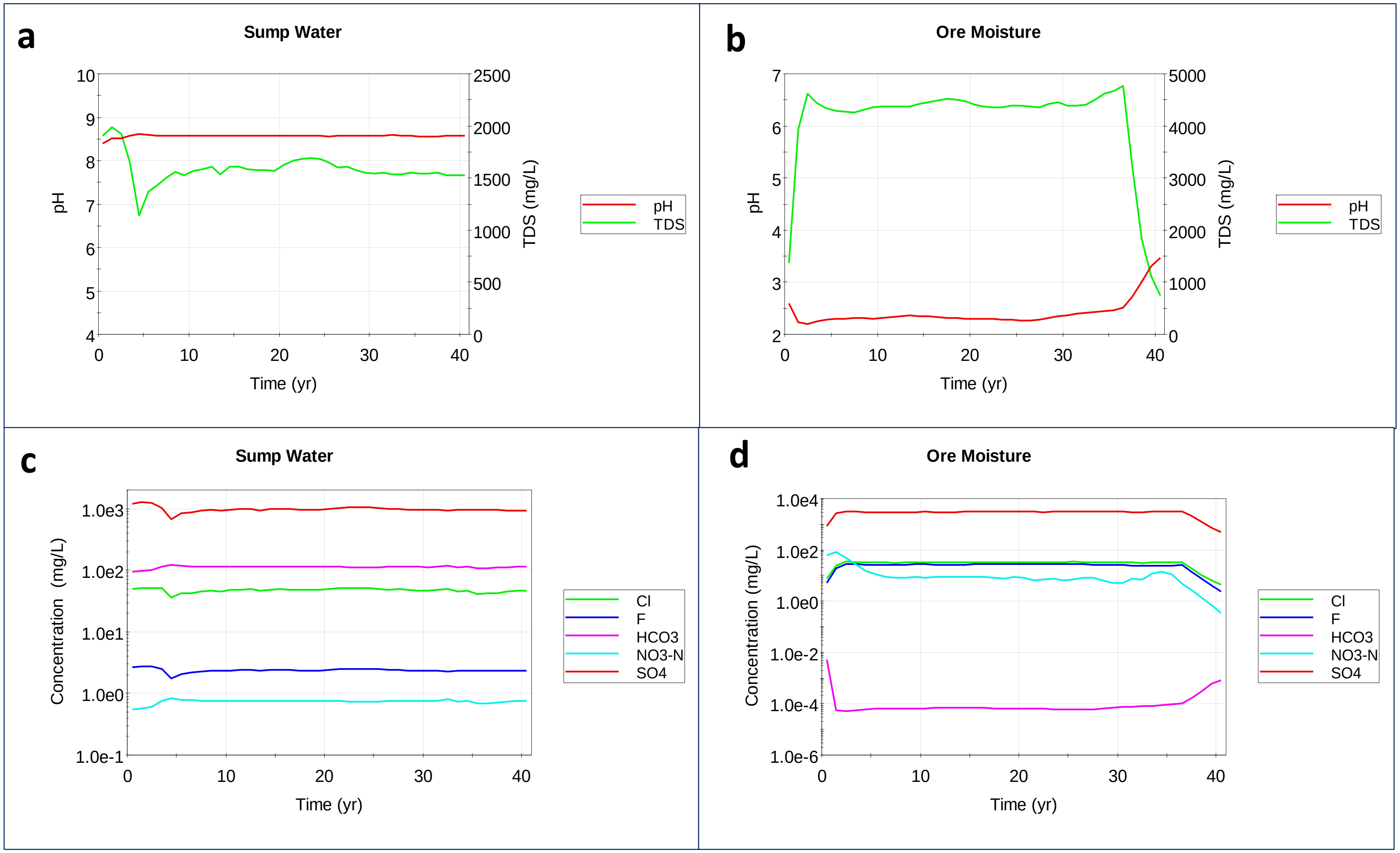

Figure 6-1. Results for a) pH of sump water, b) pH of ore moisture, c) major anions in sump water, and d) major anions in ore moisture

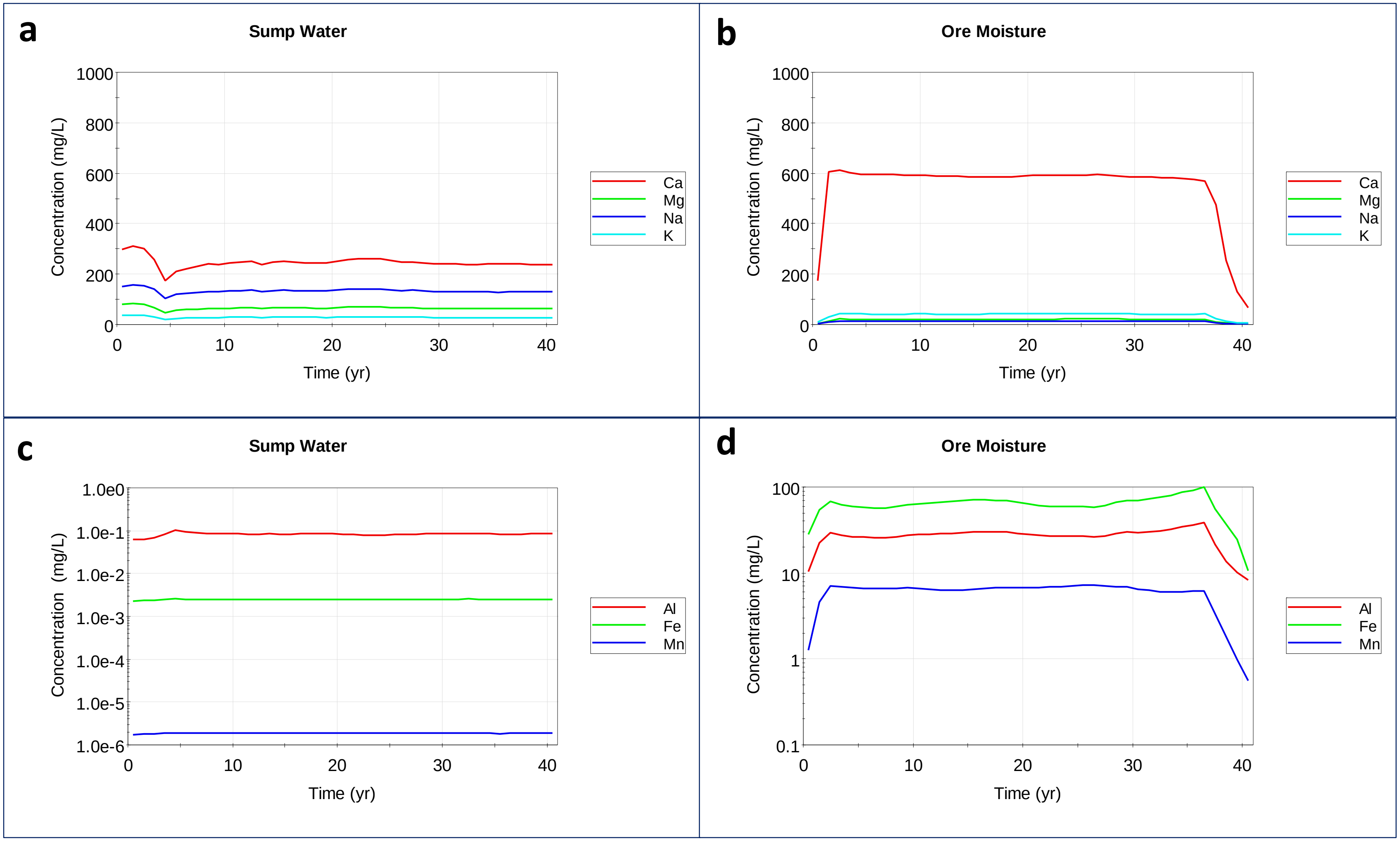

Figure 6-2. Results for a) major cations in sump water, b) major cations in ore moisture, c) Al, Fe, Mn in sump water, and d) Al, Fe, Mn in ore moisture

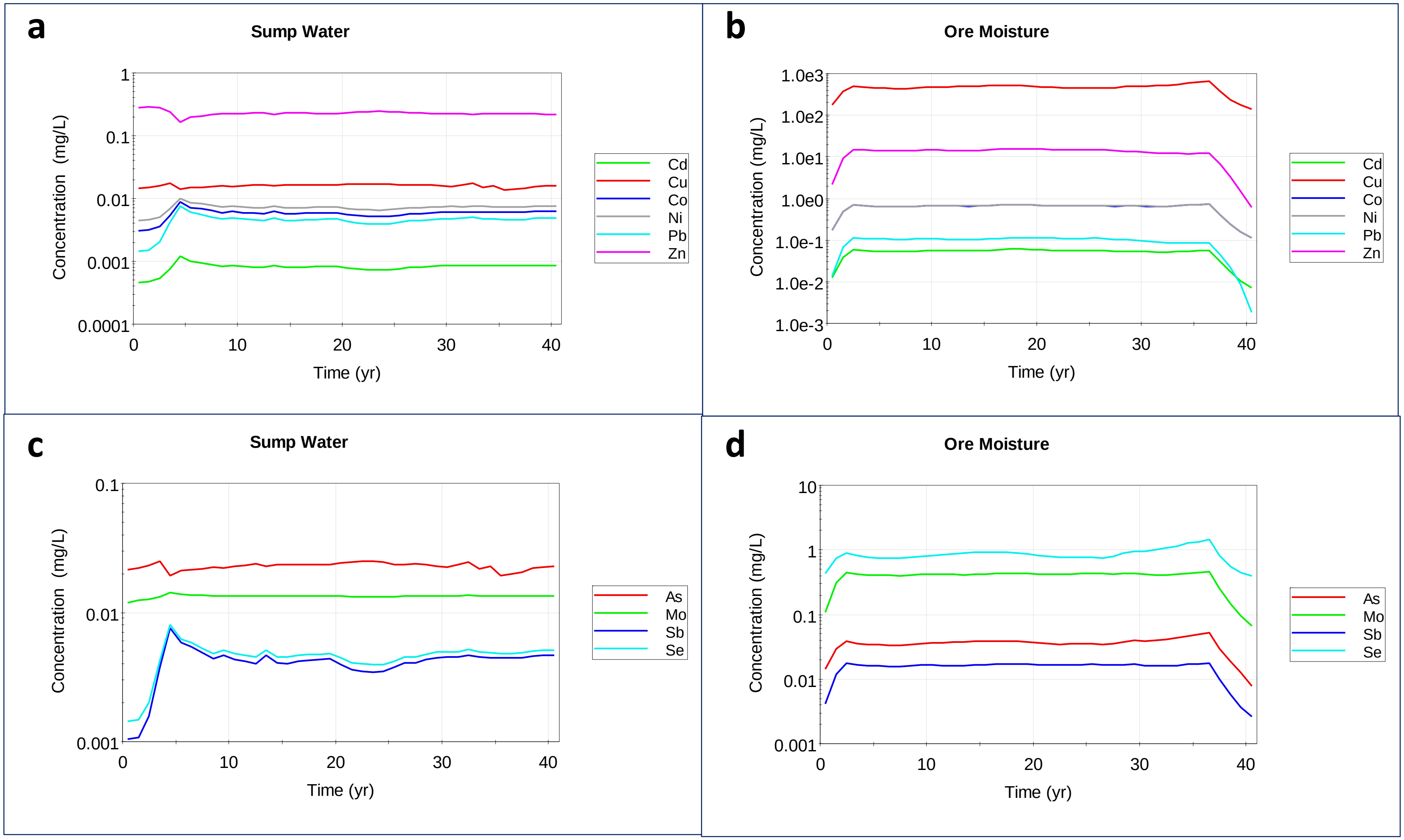

Figure 6-3. Results for a) divalent metals in sump water, b) divalent metals in ore moisture, c) As, Mo, Sb, Se in sump water, and d) As, Mo, Sb, Se in ore moisture

Table 6-1. Model results for sump water as annual average concentrations

	Ca	Mg	Na	K	Cl	HCO_3	SO_4	SiO_2	F	NO_3-N	Al	Sb	As	Ba	Be	B	Cd	Cr	Co	Cu	Fe	Pb	Mn	Mo	Ni	Se	Ag	Tl	Zn	pH	TDS
Year	mg/L	mg/L	mg/L	mg/L	mg/L	mg/L	mg/L	mg/L	mg/L	mg/L	mg/L	mg/L	mg/L	mg/L	mg/L	mg/L	mg/L	mg/L	mg/L	mg/L	mg/L	mg/L	mg/L	mg/L	mg/L	mg/L	mg/L	mg/L	mg/L	s.u.	mg/L
1	297	79	151	36	49	95	1213	21.2	2.6	0.6	6.11E-02	1.04E-03	2.14E-02	1.76E-02	1.73E-04	3.89E-01	4.57E-04	1.84E-03	3.04E-03	1.46E-02	2.30E-03	1.46E-03	1.76E-06	1.20E-02	4.43E-03	1.44E-03	4.50E-03	4.90E-04	2.80E-01	8.39	1906
2	310	83	157	37	51	99	1266	22.1	2.8	0.6	6.36E-02	1.08E-03	2.22E-02	1.84E-02	1.80E-04	4.06E-01	4.77E-04	1.91E-03	3.17E-03	1.51E-02	2.40E-03	1.51E-03	1.84E-06	1.25E-02	4.62E-03	1.49E-03	4.70E-03	5.08E-04	2.92E-01	8.51	1987
3	300	80	154	36	52	102	1218	22.2	2.8	0.6	6.72E-02	1.58E-03	2.30E-02	1.86E-02	1.94E-04	3.98E-01	5.15E-04	2.06E-03	3.60E-03	1.57E-02	2.43E-03	2.04E-03	1.85E-06	1.26E-02	5.03E-03	2.02E-03	4.57E-03	1.03E-03	2.82E-01	8.52	1925
4	256	69	139	30	52	114	1014	22.4	2.5	0.8	8.15E-02	3.76E-03	2.51E-02	1.95E-02	2.53E-04	3.61E-01	6.85E-04	2.63E-03	5.45E-03	1.74E-02	2.52E-03	4.24E-03	1.90E-06	1.33E-02	6.82E-03	4.26E-03	4.07E-03	3.31E-03	2.37E-01	8.57	1651
5	175	46	104	20	36	121	665	22.5	1.7	0.8	1.02E-01	7.59E-03	1.93E-02	2.19E-02	3.38E-04	2.87E-01	1.00E-03	3.12E-03	8.82E-03	1.38E-02	2.57E-03	7.57E-03	1.91E-06	1.42E-02	1.00E-02	7.98E-03	3.36E-03	7.37E-03	1.64E-01	8.61	1141
6	212	56	120	25	42	116	827	22.5	2.1	0.8	9.20E-02	5.83E-03	2.13E-02	2.06E-02	3.02E-04	3.20E-01	8.57E-04	2.86E-03	7.28E-03	1.49E-02	2.54E-03	6.00E-03	1.90E-06	1.38E-02	8.54E-03	6.25E-03	3.70E-03	5.51E-03	1.98E-01	8.59	1373
7	221	59	123	26	43	115	868	22.4	2.2	0.8	8.94E-02	5.38E-03	2.13E-02	2.03E-02	2.92E-04	3.28E-01	8.21E-04	2.77E-03	6.90E-03	1.49E-02	2.52E-03	5.58E-03	1.89E-06	1.37E-02	8.17E-03	5.81E-03	3.79E-03	5.04E-03	2.07E-01	8.58	1431
8	232	62	127	27	44	113	915	22.4	2.3	0.7	8.65E-02	4.87E-03	2.17E-02	2.00E-02	2.80E-04	3.38E-01	7.80E-04	2.68E-03	6.45E-03	1.52E-02	2.51E-03	5.11E-03	1.88E-06	1.35E-02	7.75E-03	5.30E-03	3.90E-03	4.49E-03	2.17E-01	8.57	1498
9	242	65	132	28	47	113	958	22.4	2.3	0.7	8.40E-02	4.39E-03	2.26E-02	1.97E-02	2.68E-04	3.47E-01	7.40E-04	2.63E-03	6.03E-03	1.57E-02	2.51E-03	4.70E-03	1.88E-06	1.34E-02	7.35E-03	4.84E-03	3.98E-03	3.99E-03	2.26E-01	8.57	1562
10	237	63	130	28	45	113	935	22.4	2.3	0.7	8.53E-02	4.64E-03	2.21E-02	1.98E-02	2.74E-04	3.42E-01	7.61E-04	2.66E-03	6.25E-03	1.54E-02	2.51E-03	4.91E-03	1.88E-06	1.35E-02	7.56E-03	5.08E-03	3.94E-03	4.26E-03	2.21E-01	8.57	1528
11	243	65	133	28	47	113	962	22.4	2.4	0.7	8.39E-02	4.34E-03	2.29E-02	1.97E-02	2.67E-04	3.48E-01	7.36E-04	2.63E-03	5.98E-03	1.59E-02	2.51E-03	4.67E-03	1.88E-06	1.34E-02	7.31E-03	4.80E-03	3.99E-03	3.94E-03	2.27E-01	8.57	1569
12	246	66	134	29	48	113	974	22.4	2.4	0.7	8.33E-02	4.21E-03	2.33E-02	1.97E-02	2.64E-04	3.51E-01	7.24E-04	2.63E-03	5.86E-03	1.62E-02	2.51E-03	4.57E-03	1.89E-06	1.34E-02	7.20E-03	4.67E-03	4.01E-03	3.80E-03	2.29E-01	8.57	1587
13	250	67	136	29	49	113	990	22.4	2.4	0.7	8.25E-02	4.03E-03	2.38E-02	1.96E-02	2.60E-04	3.55E-01	7.09E-04	2.62E-03	5.70E-03	1.65E-02	2.51E-03	4.43E-03	1.89E-06	1.34E-02	7.05E-03	4.51E-03	4.04E-03	3.61E-03	2.32E-01	8.57	1612
14	237	63	130	28	47	114	936	22.4	2.3	0.8	8.56E-02	4.63E-03	2.28E-02	1.99E-02	2.74E-04	3.43E-01	7.59E-04	2.69E-03	6.23E-03	1.58E-02	2.52E-03	4.94E-03	1.89E-06	1.35E-02	7.55E-03	5.08E-03	3.93E-03	4.24E-03	2.21E-01	8.58	1532
15	249	66	135	29	49	113	986	22.4	2.4	0.7	8.26E-02	4.08E-03	2.35E-02	1.96E-02	2.61E-04	3.54E-01	7.13E-04	2.61E-03	5.74E-03	1.63E-02	2.51E-03	4.45E-03	1.89E-06	1.34E-02	7.09E-03	4.54E-03	4.03E-03	3.65E-03	2.32E-01	8.57	1605
16	250	67	136	29	49	113	990	22.4	2.4	0.7	8.24E-02	4.04E-03	2.36E-02	1.96E-02	2.60E-04	3.54E-01	7.10E-04	2.61E-03	5.71E-03	1.64E-02	2.51E-03	4.42E-03	1.89E-06	1.34E-02	7.05E-03	4.50E-03	4.04E-03	3.61E-03	2.32E-01	8.57	1611
17	246	66	134	29	48	113	973	22.4	2.4	0.7	8.34E-02	4.22E-03	2.34E-02	1.97E-02	2.64E-04	3.51E-01	7.25E-04	2.63E-03	5.87E-03	1.62E-02	2.51E-03	4.58E-03	1.89E-06	1.34E-02	7.21E-03	4.69E-03	4.00E-03	3.81E-03	2.29E-01	8.57	1586
18	245	65	134	29	48	113	968	22.4	2.4	0.7	8.37E-02	4.27E-03	2.34E-02	1.97E-02	2.66E-04	3.50E-01	7.29E-04	2.64E-03	5.91E-03	1.62E-02	2.51E-03	4.63E-03	1.89E-06	1.34E-02	7.25E-03	4.74E-03	3.99E-03	3.86E-03	2.28E-01	8.57	1580
19	244	65	134	29	48	114	965	22.4	2.4	0.8	8.40E-02	4.30E-03	2.35E-02	1.97E-02	2.66E-04	3.50E-01	7.31E-04	2.66E-03	5.94E-03	1.63E-02	2.51E-03	4.67E-03	1.89E-06	1.34E-02	7.27E-03	4.77E-03	3.99E-03	3.89E-03	2.27E-01	8.57	1576
20	243	65	133	28	48	114	960	22.4	2.4	0.8	8.43E-02	4.37E-03	2.34E-02	1.97E-02	2.68E-04	3.48E-01	7.37E-04	2.66E-03	6.00E-03	1.62E-02	2.51E-03	4.72E-03	1.89E-06	1.34E-02	7.33E-03	4.83E-03	3.97E-03	3.96E-03	2.26E-01	8.57	1567
21	252	67	137	29	50	113	997	22.4	2.4	0.7	8.21E-02	3.95E-03	2.40E-02	1.95E-02	2.58E-04	3.56E-01	7.02E-04	2.61E-03	5.63E-03	1.66E-02	2.51E-03	4.36E-03	1.89E-06	1.33E-02	6.98E-03	4.43E-03	4.05E-03	3.52E-03	2.34E-01	8.57	1623
22	259	69	140	30	51	113	1028	22.4	2.5	0.7	8.04E-02	3.61E-03	2.46E-02	1.94E-02	2.49E-04	3.63E-01	6.74E-04	2.57E-03	5.33E-03	1.70E-02	2.51E-03	4.07E-03	1.89E-06	1.33E-02	6.70E-03	4.10E-03	4.11E-03	3.16E-03	2.40E-01	8.57	1668
23	261	70	141	31	52	112	1039	22.4	2.5	0.7	7.97E-02	3.49E-03	2.48E-02	1.94E-02	2.46E-04	3.65E-01	6.64E-04	2.56E-03	5.22E-03	1.71E-02	2.50E-03	3.97E-03	1.89E-06	1.32E-02	6.60E-03	3.98E-03	4.14E-03	3.03E-03	2.42E-01	8.57	1684
24	262	70	141	31	52	112	1043	22.4	2.5	0.7	7.95E-02	3.45E-03	2.48E-02	1.93E-02	2.45E-04	3.66E-01	6.61E-04	2.55E-03	5.19E-03	1.71E-02	2.50E-03	3.93E-03	1.89E-06	1.32E-02	6.57E-03	3.94E-03	4.14E-03	2.99E-03	2.43E-01	8.57	1689
25	261	70	141	31	52	112	1040	22.4	2.5	0.7	7.96E-02	3.49E-03	2.46E-02	1.93E-02	2.46E-04	3.65E-01	6.64E-04	2.55E-03	5.22E-03	1.70E-02	2.50E-03	3.96E-03	1.89E-06	1.32E-02	6.60E-03	3.98E-03	4.14E-03	3.03E-03	2.42E-01	8.57	1684
26	256	68	138	30	49	111	1017	22.3	2.5	0.7	8.06E-02	3.75E-03	2.34E-02	1.94E-02	2.52E-04	3.59E-01	6.88E-04	2.54E-03	5.46E-03	1.62E-02	2.50E-03	4.14E-03	1.88E-06	1.33E-02	6.82E-03	4.21E-03	4.10E-03	3.31E-03	2.38E-01	8.56	1647
27	249	66	135	29	49	113	985	22.4	2.4	0.7	8.27E-02	4.09E-03	2.34E-02	1.96E-02	2.61E-04	3.53E-01	7.15E-04	2.61E-03	5.76E-03	1.62E-02	2.51E-03	4.46E-03	1.89E-06	1.34E-02	7.10E-03	4.56E-03	4.03E-03	3.67E-03	2.31E-01	8.57	1603
28	249	67	136	29	49	113	987	22.4	2.4	0.7	8.27E-02	4.07E-03	2.38E-02	1.96E-02	2.61E-04	3.54E-01	7.12E-04	2.62E-03	5.73E-03	1.65E-02	2.51E-03	4.46E-03	1.89E-06	1.34E-02	7.08E-03	4.54E-03	4.03E-03	3.64E-03	2.31E-01	8.57	1607
29	244	65	134	29	48	114	965	22.4	2.4	0.8	8.39E-02	4.30E-03	2.34E-02	1.97E-02	2.66E-04	3.50E-01	7.31E-04	2.65E-03	5.94E-03	1.63E-02	2.51E-03	4.66E-03	1.89E-06	1.34E-02	7.27E-03	4.77E-03	3.99E-03	3.89E-03	2.27E-01	8.57	1576
30	241	64	132	28	47	113	951	22.4	2.3	0.7	8.46E-02	4.47E-03	2.29E-02	1.98E-02	2.70E-04	3.46E-01	7.45E-04	2.66E-03	6.09E-03	1.59E-02	2.51E-03	4.79E-03	1.89E-06	1.35E-02	7.41E-03	4.92E-03	3.96E-03	4.07E-03	2.24E-01	8.57	1553
31	240	64	131	28	46	113	948	22.4	2.3	0.7	8.46E-02	4.51E-03	2.23E-02	1.98E-02	2.71E-04	3.45E-01	7.50E-04	2.64E-03	6.13E-03	1.55E-02	2.51E-03	4.79E-03	1.88E-06	1.34E-02	7.45E-03	4.95E-03	3.96E-03	4.11E-03	2.24E-01	8.57	1546
32	240	64	132	28	48	114	947	22.4	2.3	0.8	8.51E-02	4.50E-03	2.34E-02	1.98E-02	2.71E-04	3.46E-01	7.47E-04	2.69E-03	6.11E-03	1.63E-02	2.52E-03	4.85E-03	1.89E-06	1.35E-02	7.44E-03	4.97E-03	3.94E-03	4.10E-03	2.23E-01	8.58	1550
33	237	64	132	28	50	117	932	22.4	2.3	0.8	8.67E-02	4.65E-03	2.47E-02	1.99E-02	2.76E-04	3.45E-01	7.57E-04	2.79E-03	6.22E-03	1.72E-02	2.54E-03	5.07E-03	1.91E-06	1.36E-02	7.55E-03	5.15E-03	3.89E-03	4.25E-03	2.19E-01	8.59	1535
34	239	63	130	28	45	112	944	22.4	2.3	0.7	8.45E-02	4.55E-03	2.16E-02	1.98E-02	2.72E-04	3.43E-01	7.55E-04	2.61E-03	6.18E-03	1.51E-02	2.50E-03	4.80E-03	1.87E-06	1.34E-02	7.49E-03	4.98E-03	3.96E-03	4.16E-03	2.23E-01	8.57	1538
35	241	64	132	28	47	113	952	22.4	2.3	0.7	8.45E-02	4.46E-03	2.27E-02	1.98E-02	2.70E-04	3.46E-01	7.45E-04	2.65E-03	6.08E-03	1.58E-02	2.51E-03	4.77E-03	1.88E-06	1.34E-02	7.41E-03	4.91E-03	3.97E-03	4.06E-03	2.25E-01	8.57	1554
36	240	64	128	28	41	107	957	22.3	2.4	0.7	8.25E-02	4.45E-03	1.93E-02	1.97E-02	2.68E-04	3.43E-01	7.51E-04	2.46E-03	6.11E-03	1.34E-02	2.47E-03	4.55E-03	1.84E-06	1.34E-02	7.41E-03	4.81E-03	4.03E-03	4.06E-03	2.27E-01	8.55	1546
37	240	64	129	28	42	108	955	22.3	2.3	0.7	8.29E-02	4.46E-03	1.98E-02	1.97E-02	2.69E-04	3.43E-01	7.50E-04	2.49E-03	6.12E-03	1.38E-02	2.47E-03	4.59E-03	1.85E-06	1.34E-02	7.41E-03	4.83E-03	4.02E-03	4.07E-03	2.27E-01	8.55	1546
38	240	64	130	28	43	109	955	22.3	2.3	0.7	8.33E-02	4.45E-03	2.05E-02	1.97E-02	2.69E-04	3.44E-01	7.49E-04	2.53E-03	6.10E-03	1.43E-02	2.48E-03	4.64E-03	1.86E-06	1.34E-02	7.41E-03	4.85E-03	4.01E-03	4.06E-03	2.26E-01	8.56	1548
39	237	63	130	28	45	112	937	22.4	2.3	0.7	8.51E-02	4.63E-03	2.19E-02	1.98E-02	2.74E-04	3.42E-01	7.60E-04	2.64E-03	6.24E-03	1.53E-02	2.51E-03	4.89E-03	1.88E-06	1.35E-02	7.55E-03	5.06E-03	3.94E-03	4.24E-03	2.22E-01	8.57	1530
40	237	63	130	28	46	113	935	22.4	2.3	0.7	8.55E-02	4.64E-03	2.25E-02	1.99E-02	2.74E-04	3.43E-01	7.60E-04	2.67E-03	6.24E-03	1.56E-02	2.51E-03	4.93E-03	1.88E-06	1.35E-02	7.56E-03	5.09E-03	3.93E-03	4.25E-03	2.21E-01	8.57	1530
41	237	63	130	28	46	114	934	22.4	2.3	0.8	8.57E-02	4.66E-03	2.27E-02	1.99E-02	2.75E-04	3.42E-01	7.61E-04	2.69E-03	6.25E-03	1.58E-02	2.52E-03	4.96E-03	1.89E-06	1.35E-02	7.57E-03	5.11E-03	3.92E-03	4.27E-03	2.21E-01	8.58	1528

Table 6-2. Model results for ore moisture as annual average concentrations

	Ca	Mg	Na	K	Cl	HCO_3	SO_4	SiO_2	F	NO_3-N	Al	Sb	As	Ba	Be	B	Cd	Cr	Co	Cu	Fe	Pb	Mn	Mo	Ni	Se	Ag	Tl	Zn	pH	TDS
Year	mg/L	mg/L	mg/L	mg/L	mg/L	mg/L	mg/L	mg/L	mg/L	mg/L	mg/L	mg/L	mg/L	mg/L	mg/L	mg/L	mg/L	mg/L	mg/L	mg/L	mg/L	mg/L	mg/L	mg/L	mg/L	mg/L	mg/L	mg/L	mg/L	s.u.	mg/L
1	174	4	3	9	8	0	872	19.7	5.2	60.1	1.04E+01	4.16E-03	1.44E-02	2.12E-02	1.60E-02	7.99E-02	1.24E-02	1.11E-01	1.73E-01	1.77E+02	2.84E+01	1.37E-02	1.26E+00	1.07E-01	1.75E-01	4.33E-01	6.89E-02	1.10E-03	2.16E+00	2.59	1379
2	604	15	10	30	23	0	2656	20.4	18.7	81.2	2.24E+01	1.20E-02	2.99E-02	1.76E-02	4.62E-02	2.32E-01	3.93E-02	3.12E-01	4.85E-01	3.83E+02	5.42E+01	6.81E-02	4.62E+00	3.07E-01	4.90E-01	7.52E-01	1.95E-01	3.07E-03	9.39E+00	2.24	3938
3	611	23	15	45	35	0	3174	20.4	28.6	47.8	2.96E+01	1.74E-02	3.85E-02	1.67E-02	6.71E-02	3.38E-01	5.86E-02	4.50E-01	6.98E-01	5.04E+02	6.74E+01	1.11E-01	7.10E+00	4.44E-01	7.05E-01	8.91E-01	2.81E-01	4.41E-03	1.49E+01	2.19	4628
4	601	22	14	43	33	0	3067	20.4	27.7	25.2	2.76E+01	1.66E-02	3.58E-02	1.66E-02	6.42E-02	3.24E-01	5.64E-02	4.30E-01	6.67E-01	4.71E+02	6.21E+01	1.09E-01	6.88E+00	4.25E-01	6.73E-01	8.08E-01	2.68E-01	4.21E-03	1.46E+01	2.25	4443
5	597	21	14	42	32	0	3002	20.4	26.9	15.0	2.65E+01	1.61E-02	3.43E-02	1.65E-02	6.22E-02	3.14E-01	5.48E-02	4.16E-01	6.45E-01	4.52E+02	5.92E+01	1.06E-01	6.69E+00	4.11E-01	6.52E-01	7.66E-01	2.60E-01	4.08E-03	1.43E+01	2.28	4336
6	595	21	14	42	32	0	2982	20.4	26.7	10.8	2.61E+01	1.60E-02	3.38E-02	1.65E-02	6.17E-02	3.11E-01	5.44E-02	4.12E-01	6.39E-01	4.46E+02	5.82E+01	1.06E-01	6.65E+00	4.08E-01	6.46E-01	7.50E-01	2.57E-01	4.04E-03	1.42E+01	2.29	4300
7	594	21	14	41	32	0	2962	20.4	26.5	8.9	2.58E+01	1.58E-02	3.33E-02	1.65E-02	6.10E-02	3.07E-01	5.38E-02	4.07E-01	6.32E-01	4.40E+02	5.73E+01	1.05E-01	6.58E+00	4.03E-01	6.38E-01	7.38E-01	2.54E-01	3.99E-03	1.41E+01	2.30	4269
8	594	21	14	41	32	0	2954	20.4	26.3	8.4	2.57E+01	1.57E-02	3.32E-02	1.65E-02	6.07E-02	3.06E-01	5.36E-02	4.05E-01	6.29E-01	4.38E+02	5.71E+01	1.05E-01	6.54E+00	4.01E-01	6.35E-01	7.36E-01	2.53E-01	3.97E-03	1.40E+01	2.31	4257
9	593	21	14	42	32	0	2987	20.4	26.9	8.0	2.65E+01	1.60E-02	3.42E-02	1.64E-02	6.20E-02	3.13E-01	5.48E-02	4.14E-01	6.44E-01	4.52E+02	5.93E+01	1.06E-01	6.64E+00	4.10E-01	6.50E-01	7.64E-01	2.59E-01	4.06E-03	1.43E+01	2.31	4308
10	592	21	14	42	33	0	3020	20.4	27.3	8.6	2.73E+01	1.64E-02	3.52E-02	1.64E-02	6.33E-02	3.19E-01	5.59E-02	4.23E-01	6.58E-01	4.66E+02	6.16E+01	1.08E-01	6.70E+00	4.18E-01	6.63E-01	7.96E-01	2.64E-01	4.15E-03	1.46E+01	2.30	4361
11	590	21	14	42	33	0	3030	20.4	27.3	8.0	2.78E+01	1.64E-02	3.59E-02	1.64E-02	6.36E-02	3.20E-01	5.61E-02	4.25E-01	6.63E-01	4.76E+02	6.34E+01	1.08E-01	6.66E+00	4.20E-01	6.67E-01	8.23E-01	2.65E-01	4.17E-03	1.46E+01	2.31	4380
12	590	21	14	41	32	0	3018	20.4	26.8	8.6	2.81E+01	1.63E-02	3.63E-02	1.64E-02	6.29E-02	3.17E-01	5.55E-02	4.21E-01	6.57E-01	4.80E+02	6.48E+01	1.05E-01	6.48E+00	4.15E-01	6.61E-01	8.46E-01	2.63E-01	4.13E-03	1.43E+01	2.33	4372
13	589	20	14	41	32	0	3020	20.4	26.6	8.9	2.86E+01	1.62E-02	3.70E-02	1.64E-02	6.28E-02	3.16E-01	5.53E-02	4.21E-01	6.58E-01	4.89E+02	6.69E+01	1.03E-01	6.36E+00	4.14E-01	6.61E-01	8.78E-01	2.62E-01	4.13E-03	1.42E+01	2.34	4383
14	588	20	14	40	32	0	3014	20.4	26.3	8.5	2.88E+01	1.61E-02	3.73E-02	1.64E-02	6.24E-02	3.14E-01	5.50E-02	4.19E-01	6.55E-01	4.94E+02	6.80E+01	1.02E-01	6.25E+00	4.11E-01	6.58E-01	8.96E-01	2.61E-01	4.11E-03	1.41E+01	2.35	4380
15	587	20	14	41	32	0	3045	20.4	26.8	8.6	2.96E+01	1.64E-02	3.83E-02	1.64E-02	6.36E-02	3.20E-01	5.61E-02	4.27E-01	6.69E-01	5.07E+02	7.01E+01	1.03E-01	6.32E+00	4.19E-01	6.71E-01	9.24E-01	2.66E-01	4.19E-03	1.43E+01	2.35	4428
16	586	21	14	42	33	0	3069	20.4	27.3	8.6	3.00E+01	1.67E-02	3.87E-02	1.63E-02	6.46E-02	3.26E-01	5.73E-02	4.34E-01	6.80E-01	5.14E+02	7.09E+01	1.06E-01	6.42E+00	4.26E-01	6.82E-01	9.32E-01	2.70E-01	4.25E-03	1.47E+01	2.35	4464
17	587	21	14	42	33	0	3090	20.4	28.0	8.8	3.01E+01	1.69E-02	3.87E-02	1.63E-02	6.55E-02	3.30E-01	5.87E-02	4.39E-01	6.91E-01	5.16E+02	7.06E+01	1.10E-01	6.55E+00	4.31E-01	6.92E-01	9.21E-01	2.73E-01	4.30E-03	1.52E+01	2.33	4490
18	587	21	15	43	34	0	3113	20.4	28.7	8.4	3.02E+01	1.72E-02	3.87E-02	1.63E-02	6.65E-02	3.35E-01	6.03E-02	4.45E-01	7.02E-01	5.19E+02	7.04E+01	1.15E-01	6.69E+00	4.38E-01	7.03E-01	9.10E-01	2.77E-01	4.36E-03	1.57E+01	2.32	4519
19	587	22	15	43	34	0	3109	20.4	28.8	7.5	2.99E+01	1.72E-02	3.82E-02	1.63E-02	6.65E-02	3.35E-01	6.02E-02	4.45E-01	7.01E-01	5.13E+02	6.90E+01	1.16E-01	6.77E+00	4.38E-01	7.02E-01	8.89E-01	2.77E-01	4.36E-03	1.57E+01	2.31	4507
20	589	22	15	43	34	0	3088	20.4	28.5	9.1	2.90E+01	1.70E-02	3.72E-02	1.64E-02	6.57E-02	3.31E-01	5.92E-02	4.39E-01	6.90E-01	4.97E+02	6.64E+01	1.14E-01	6.80E+00	4.33E-01	6.92E-01	8.54E-01	2.74E-01	4.30E-03	1.55E+01	2.30	4469
21	590	21	14	43	33	0	3055	20.4	28.0	8.1	2.81E+01	1.67E-02	3.60E-02	1.64E-02	6.46E-02	3.26E-01	5.79E-02	4.32E-01	6.75E-01	4.80E+02	6.35E+01	1.12E-01	6.79E+00	4.26E-01	6.79E-01	8.16E-01	2.69E-01	4.23E-03	1.52E+01	2.30	4413
22	591	21	14	43	33	0	3035	20.4	27.8	6.7	2.74E+01	1.65E-02	3.52E-02	1.64E-02	6.40E-02	3.23E-01	5.70E-02	4.28E-01	6.66E-01	4.67E+02	6.14E+01	1.11E-01	6.82E+00	4.22E-01	6.71E-01	7.87E-01	2.67E-01	4.19E-03	1.50E+01	2.30	4376
23	592	21	14	43	33	0	3021	20.4	27.5	7.1	2.69E+01	1.64E-02	3.47E-02	1.64E-02	6.35E-02	3.20E-01	5.60E-02	4.24E-01	6.58E-01	4.58E+02	6.00E+01	1.09E-01	6.85E+00	4.20E-01	6.64E-01	7.70E-01	2.65E-01	4.16E-03	1.47E+01	2.29	4351
24	592	22	14	43	33	0	3034	20.4	27.7	7.5	2.69E+01	1.66E-02	3.48E-02	1.64E-02	6.41E-02	3.24E-01	5.62E-02	4.29E-01	6.62E-01	4.58E+02	5.98E+01	1.10E-01	6.97E+00	4.24E-01	6.70E-01	7.68E-01	2.68E-01	4.20E-03	1.47E+01	2.28	4367
25	592	22	15	44	34	0	3050	20.4	28.0	6.7	2.70E+01	1.68E-02	3.51E-02	1.64E-02	6.49E-02	3.28E-01	5.66E-02	4.34E-01	6.69E-01	4.59E+02	5.98E+01	1.11E-01	7.11E+00	4.30E-01	6.77E-01	7.69E-01	2.71E-01	4.25E-03	1.48E+01	2.28	4386
26	593	22	15	45	34	0	3056	20.4	28.1	7.1	2.69E+01	1.69E-02	3.50E-02	1.64E-02	6.52E-02	3.29E-01	5.67E-02	4.36E-01	6.70E-01	4.57E+02	5.92E+01	1.11E-01	7.21E+00	4.32E-01	6.80E-01	7.61E-01	2.72E-01	4.27E-03	1.48E+01	2.27	4392
27	594	22	15	45	34	0	3045	20.4	27.7	8.1	2.66E+01	1.68E-02	3.47E-02	1.65E-02	6.48E-02	3.27E-01	5.58E-02	4.33E-01	6.63E-01	4.51E+02	5.84E+01	1.09E-01	7.21E+00	4.29E-01	6.74E-01	7.54E-01	2.70E-01	4.24E-03	1.46E+01	2.27	4374
28	593	22	14	44	34	0	3032	20.4	27.0	8.1	2.70E+01	1.66E-02	3.56E-02	1.64E-02	6.40E-02	3.23E-01	5.45E-02	4.29E-01	6.56E-01	4.57E+02	6.05E+01	1.04E-01	7.04E+00	4.24E-01	6.67E-01	7.98E-01	2.68E-01	4.21E-03	1.39E+01	2.29	4366
29	589	22	14	44	34	0	3059	20.4	26.8	6.4	2.86E+01	1.68E-02	3.79E-02	1.64E-02	6.48E-02	3.26E-01	5.47E-02	4.35E-01	6.67E-01	4.85E+02	6.59E+01	1.01E-01	6.95E+00	4.30E-01	6.78E-01	8.89E-01	2.72E-01	4.28E-03	1.37E+01	2.31	4422
30	585	22	14	43	34	0	3077	20.4	26.5	5.3	2.98E+01	1.69E-02	3.98E-02	1.63E-02	6.52E-02	3.28E-01	5.48E-02	4.39E-01	6.74E-01	5.07E+02	7.02E+01	9.84E-02	6.84E+00	4.33E-01	6.84E-01	9.61E-01	2.74E-01	4.32E-03	1.34E+01	2.34	4461
31	586	21	14	42	32	0	3027	20.4	25.5	5.3	2.93E+01	1.63E-02	3.91E-02	1.63E-02	6.30E-02	3.17E-01	5.31E-02	4.24E-01	6.53E-01	4.98E+02	6.95E+01	9.43E-02	6.52E+00	4.18E-01	6.63E-01	9.57E-01	2.65E-01	4.17E-03	1.29E+01	2.36	4396
32	585	20	14	41	32	0	3017	20.4	24.8	7.6	2.99E+01	1.61E-02	4.00E-02	1.63E-02	6.21E-02	3.12E-01	5.23E-02	4.18E-01	6.47E-01	5.09E+02	7.21E+01	9.05E-02	6.28E+00	4.12E-01	6.55E-01	1.00E+00	2.61E-01	4.12E-03	1.24E+01	2.39	4397
33	583	19	14	40	31	0	3017	20.4	24.3	7.3	3.07E+01	1.60E-02	4.12E-02	1.63E-02	6.17E-02	3.10E-01	5.18E-02	4.17E-01	6.46E-01	5.24E+02	7.54E+01	8.72E-02	6.09E+00	4.10E-01	6.54E-01	1.06E+00	2.60E-01	4.11E-03	1.21E+01	2.42	4411
34	583	20	14	40	32	0	3065	20.4	24.4	12.1	3.24E+01	1.63E-02	4.36E-02	1.63E-02	6.31E-02	3.16E-01	5.27E-02	4.27E-01	6.63E-01	5.52E+02	8.07E+01	8.59E-02	6.08E+00	4.19E-01	6.71E-01	1.15E+00	2.66E-01	4.21E-03	1.20E+01	2.42	4500
35	580	20	14	41	32	0	3130	20.4	24.7	13.8	3.47E+01	1.69E-02	4.70E-02	1.62E-02	6.51E-02	3.27E-01	5.39E-02	4.42E-01	6.88E-01	5.93E+02	8.82E+01	8.43E-02	6.08E+00	4.33E-01	6.95E-01	1.27E+00	2.76E-01	4.37E-03	1.19E+01	2.44	4617
36	576	20	15	41	33	0	3169	20.4	25.0	11.1	3.61E+01	1.72E-02	4.89E-02	1.62E-02	6.66E-02	3.34E-01	5.49E-02	4.53E-01	7.05E-01	6.17E+02	9.23E+01	8.41E-02	6.14E+00	4.43E-01	7.12E-01	1.33E+00	2.82E-01	4.48E-03	1.20E+01	2.46	4680
37	569	20	15	43	34	0	3230	20.4	25.4	4.7	3.83E+01	1.79E-02	5.22E-02	1.61E-02	6.90E-02	3.45E-01	5.65E-02	4.70E-01	7.32E-01	6.55E+02	9.91E+01	8.37E-02	6.22E+00	4.59E-01	7.40E-01	1.45E+00	2.93E-01	4.65E-03	1.20E+01	2.51	4780
38	474	11	8.2	23	19	0	2168	20.5	13.9	2.7	2.14E+01	9.84E-03	2.92E-02	1.69E-02	3.80E-02	1.90E-01	3.10E-02	2.59E-01	4.04E-01	3.66E+02	5.58E+01	4.51E-02	3.38E+00	2.53E-01	4.08E-01	8.17E-01	1.61E-01	2.57E-03	6.51E+00	2.73	3199
39	255	6	4.7	13	11	0	1226	20.6	7.5	1.4	1.36E+01	5.72E-03	1.88E-02	1.87E-02	2.21E-02	1.10E-01	1.74E-02	1.52E-01	2.37E-01	2.33E+02	3.67E+01	2.17E-02	1.81E+00	1.47E-01	2.39E-01	5.52E-01	9.43E-02	1.51E-03	3.28E+00	3.01	1838
40	131	3.5	3.0	8	6.6	0	730	19.7	4.1	0.7	1.01E+01	3.69E-03	1.27E-02	2.08E-02	1.40E-02	7.05E-02	1.05E-02	9.88E-02	1.55E-01	1.74E+02	2.46E+01	8.55E-03	9.83E-01	9.50E-02	1.57E-01	4.46E-01	6.15E-02	9.91E-04	1.52E+00	3.31	1122
41	68	2.1	2.1	5	4.5	0	474	15.2	2.4	0.4	8.36E+00	2.65E-03	7.86E-03	2.34E-02	9.30E-03	5.03E-02	7.01E-03	7.14E-02	1.13E-01	1.43E+02	1.07E+01	1.86E-03	5.59E-01	6.71E-02	1.15E-01	3.91E-01	4.47E-02	7.27E-04	6.15E-01	3.46	742

7 REFERENCES

AZ (2016) Arizona Water Company, 2016 Annual Water Quality Report for Superior, Arizona, PWSID NO. 11-021.

Bailey, B.L., L.J.D. Smith, D.W. Blowes, C.J. Ptacek, L. Smith, and D.C. Sego (2011) Diavik waste rock project: residuals in waste rock piles. Proceedings Tailings and Mine Waste 2011, Vancouver, BC, Nov. t to 9, 2011.

Eary, T. (2007) Linking GoldSim with the PHREEQC Geochemical Model with a Dynamic Link Library. 2007 GoldSim User's Conference, San Francisco, CA.

Enchemica (2018a) Block cave water balance – 2018 Update. Technical Memo to H. Gluski (Resolution Copper) from T. Eary (Enchemica), April 2018.

Enchemica (2018b) Oxidation Zone Thickness for Draw-Points in the Block Cave Mine – 2018 Update. Technical Memo to H. Gluski (Resolution Copper) from T. Eary (Enchemica), May 2018.

Ferguson, K.D. and S. M. Leask (1988) The export of nutrients from surface coal mines. Regional Program Report 87-12, Environment Canada, March 1988.

Hatch (2016) Prediction of Block Cave Water Chemistry. Final Draft Report. Resolution Copper Mining, Resolution Project Geochemistry. Prepared by Hatch (H349053-00000-121-066-0001), Fort Collins, Colorado, January 8, 2016.

Hem, J.D. (1989) Study and Interpretation of the Chemical Characteristics of Natural Water, Third Edition. U.S. Geological Survey Water Supply Paper 2254, U.S. Government Printing Office, Washington, D.C.

Labrecque (2017) Underground Ore Residence Time Analysis, Resolution Copper Mining. Report by Labrecque Technologies, Inc., May 15, 2017.

McKibben, M.A. and H.L. Barnes (1986) Oxidation of pyrite in low temperature acidic solutions: Rate laws and surface textures. Geochim. Cosmochim. Acta 50, 1509-1520.

Moreby, R. (2018) Resolution Project - Drawpoint Rock Pile Temperatures. Draft Report prepared by R. Moreby, Morvent Mining Ltd., Plymouth, United Kingdom; Prepared for Resolution Copper, January 20, 2018.

MWH (2013) Geochemical Characterization Data Summary Report. Prepared for Resolution Copper Mining; Prepared by MWH Americas, Inc., Fort Collins, Colorado.

Palandri, J.L. and Y.K. Kharaka (2004) A compilation of rate parameters of water-mineral interaction kinetics for application to geochemical modeling. U.S. Geological Survey Open File Report 2004-1068, U.S. Geol. Survey Information Center, Denver, Colorado.

Parkhurst, D.L. and Appelo, C.A.J. (2013) Description of Input and Examples for PHREEQC Version 3 – A Computer Program for Speciation, Batch-Reaction, One-Dimensional Transport, and Inverse Geochemical Calculations. U.S. Geological Survey Techniques and Methods, Book 6, Chapter A43, 497 p, available only at http://pubs.usgs.gov/tm/06/a43.

RC (2016) General Plan of Operations. Resolution Copper Mining, May 9, 2016.

RC (2017) Underground Operations Inputs to Geochemical Modeling. Resolution Copper Technical Memo from A. Luke to T. Eary, H. Gluski, V. Peacey, M. Groulx, and B. Mead. Draft, August 2, 2017.

WSP (2018) Groundwater hydrology modeling report – to be completed. File: 180314b_PA_LOM_FlowsForGeochemistry.xlsx

102 Magma Heights – P.O. Box 1944
Superior, AZ 85173
Tel.: 520.689.9374
Fax: 520.689.9304

June 27, 2018

Ms. Mary Rasmussen
US Forest Service
Supervisor's Office
2324 East McDowell Road
Phoenix, AZ 85006-2496

Subject: Response to Analysis Data Request #1 – Request for Analysis of Tailings Seepage – Item #1.

Dear Ms. Rasmussen,

In partial response to your letter dated March 8, 2018, the following document is attached as requested:

1. **Block-cave geochemical modeling**. It is our understanding that the geochemical modeling for the block cave zone is being updated, with an expectation that modeling would cover both operational and post-closure time frames.

Request: RCM to provide USFS with block cave geochemical modeling.

RCM Response: As requested, please see the attached technical memorandum by Enchemica dated June 26, 2018 titled "Block Cave Geochemical Model - 2018 Update on Calculation Approach and Results.

Sincerely,

Vicky Peacey,

Senior Manager, Environment, Permitting and Approvals; Resolution Copper Company, as Manager of Resolution Copper Mining, LLC

Cc: Ms. Mary Morissette; Senior Environmental Specialist; Resolution Copper Company

Enclosure(s)

Technical Memorandum by Enchemica (2018), Block Cave Geochemical Model - 2018 Update on Calculation Approach and Results